Analysis of Alternative Modifications for Reducing Backwater at the Interstate Highway 10 Crossing of the Pearl River Near Slidell, Louisiana

United States Geological Survey Water-Supply Paper 2267

Prepared in cooperation with the Louisiana Department of Transportation and Development Office of Highways and the U.S. Department of Transportation Federal Highway Administration

Analysis of Alternative Modifications for Reducing Backwater at the Interstate Highway 10 Crossing of the Pearl River Near Slidell, Louisiana

By GREGG J. WICHE, J. J. GILBERT,
DAVID C. FROEHLICH, and JONATHAN K. LEE

Prepared in cooperation
with the Louisiana Department
of Transportation and Development
Office of Highways and the U.S.
Department of Transportation
Federal Highway Administration

U.S. GEOLOGICAL SURVEY WATER-SUPPLY PAPER 2267

DEPARTMENT OF THE INTERIOR
DONALD PAUL HODEL, Secretary

U.S. GEOLOGICAL SURVEY
Dallas L. Peck, Director

UNITED STATES GOVERNMENT PRINTING OFFICE 1988

For sale by the Books and Open-File Reports Section,
U S Geological Survey, Federal Center,
Box 25425, Denver, CO 80225

Library of Congress Cataloging in Publication Data

Analysis of alternative modifications for reducing backwater at the Interstate Highway 10 crossing of the Pearl River near Slidell, Louisiana
(U S Geological Survey water-supply paper , 2267)
"Prepared in cooperation with the Louisiana Department of Transportation and Development, Office of Highways and the U S Department of Transportation, Federal Highway Administration"
Bibliography p
Supt of Docs no I 19 13 2267
1 Floods—Pearl River (Miss and La) 2 Backwater 3 Interstate 10 4 Flood damage prevention—Louisiana—Slidell Region I Wiche, Gregg J II Louisiana Office of Highways III United States Federal Highway Administration IV Series
TC425 P4A53 1988 627' 4'0976312 87-600499

CONTENTS

PLATES [Plates are at back of report]

FIGURES

TABLES

Analysis of Alternative Modifications for Reducing Backwater at the Interstate Highway 10 Crossing of the Pearl River near Slidell, Louisiana

By Gregg J. Wiche, J. J. Gilbert, David C. Froehlich, *and* Jonathan K. Lee

Abstract

In April 1979 and April 1980, major flooding along the lower Pearl River caused extensive damage to homes located on the flood plain in the Slidell, Louisiana, area In response to questions about causes of these floods and means of mitigating future floods, the U S Geological Survey, in cooperation with the Louisiana Department of Transportation and Development, Office of Highways, and the U S Department of Transportation, Federal Highway Administration, used a two-dimensional finite-element surface-water flow-modeling system to study the effect of four alternative modifications for improving the hydraulic characteristics of the Interstate Highway 10 crossing of the flood plain near Slidell The analysis used the model's capability to simulate changes in flood-plain topography, flood-plain vegetative cover, and highway-embankment geometry

Compared with the existing highway crossing, the four alternative modifications reduce backwater and average velocities through bridge openings for a flood of the magnitude of the 1980 flood The four alternatives also eliminate roadway overtopping during such a flood For the four modifications, maximum backwater on the west side of the flood plain ranges from 0 3 to 1 1 feet and on the east side from 0 3 to 0 7 foot Results of the alternative-model simulations show that backwater is greater on the west side of the flood plain than on the east side, but upstream from Interstate Highway 10 backwater decreases more rapidly in the upstream direction on the west side of the flood plain than on the east side Downstream from Interstate Highway 10, modeling of the four alternatives indicates that backwater and drawdown still occur on the east and west sides of the flood plain, respectively, but are less than the values computed for the April 1980 flood with Interstate Highway 10 in place

In addition to other highway-crossing modifications, alternatives 2 and 3 include simulation of a new 2,000-foot bridge opening, and alternative 4 includes simulation of a 1,000-foot bridge opening The new bridge conveys 25, 23, and 21 percent of the total computed discharge in alternatives 2, 3, and 4, respectively The average velocity through the new bridge is 2 0, 1 9, and 3 4 feet per second for alternatives 2, 3, and 4, respectively

INTRODUCTION

In April 1979 and April 1980, major flooding along the lower Pearl River caused extensive damage to homes on the flood plain in the Slidell, La , area Many residents were forced from their homes until the floodwaters receded Property damages in the Slidell area due to the 1980 flood, the largest flood of record in the area to that time, were estimated to be $12.275 million (U.S. Army Corps of Engineers, 1981, p. 76). The 1980 flood forced the closing of the Interstate Highway 10 (I-10) crossing of the Pearl River flood plain between Slidell and Bay St Louis, Miss., for several hours while the flood crest passed. Many local residents attributed part of the 1979 and 1980 flooding in the Slidell area to backwater caused by the I-10 embankments.

Because of the interest in the impact of I-10 and because the April 2, 1980, flood was slightly larger than a 50-year design flood, the U S. Geological Survey, in cooperation with the Louisiana Department of Transportation and Development, Office of Highways, and the U.S. Department of Transportation, Federal Highway Administration, completed a study to determine the effect of the I-10 crossing on water-surface elevations and flow distribution during the April 1980 flood (Lee and others, 1983). On the basis of observations made during model calibration by Lee and others (1983), results obtained with a local model of the area near the West Pearl River opening in I-10, and discussions with the Office of Highways, four alternative modifications of the I-10 crossing for reducing backwater were selected for analysis in a second study This report documents the results of the second study.

The two-dimensional finite-element surface-water flow-modeling system, FESWMS, was used in this second study, for two reasons (1) the model allows simulation of steady-state flow with both lateral and longitudinal variations in velocity and water-surface elevation, and (2)

the model has been used successfully by other investigators In their study of the lower Pearl River, Lee and others (1983) demonstrated the capability of the modeling system to simulate the significant features of steady-state flow, in a complex multichannel river floodplain system having variable topography and vegetative cover. In addition, they showed that the model can simulate lateral and longitudinal variations in velocities and water-surface elevation and can easily accommodate geometric features such as highway embankments and channel bends

An earlier version of FESWMS was used by Lee (1980) and by Lee and Bennett (1981) to study the impact of a proposed highway crossing on flood stages of the Congaree River near Columbia, S C. The modeling system was used to simulate the effects of geometric features such as spur dikes and levees

Purpose and Scope

The principal objective of this study was to analyze four proposed modifications of the I-10 crossing to determine whether they reduce backwater, eliminate roadway overtopping, and reduce velocities through bridge openings for a flood of the magnitude of the April 1980 flood. Constrictions of the Pearl River flood plain created by highway embankments, together with other physical features of the flood plain, caused significant lateral variations in water-surface elevation and flow distribution during the 1980 flood. Thus, use of a two-dimensional model was warranted in order to obtain a more precise evaluation of water-surface elevations and flow distribution near the I-10 crossing than could be obtained by one-dimensional step-backwater and conveyance techniques

This report presents the application of FESWMS to the lower Pearl River and illustrates the usefulness of the two-dimensional model in studying alternative modifications of highway crossings. The report begins with a description of the study area, a discussion of Pearl River basin hydrology, and a brief description of the modeling system Data collection and network design are described. Results of the work by Lee and others (1983) are summarized, including a discussion of the results of the simulations with and without the I-10 embankments in place. Results from seven simulations using a local model centered on the West Pearl River opening at I-10 are discussed. Results of simulations of the four alternative modifications of the I-10 crossing are presented, including a discussion of the discharge distribution and backwater caused by each of the four proposed modifications Throughout the report, emphasis is on documenting flooding on the west side of the Pearl River flood plain, where most of the flood damage occurred.

Definition of Terms

Throughout this report the terms "full study reach," "full study area," "study reach," "study area," "local network," and "local model" are used repeatedly. The term "full study reach" or "full study area" refers to the 12-mi-long reach modeled by Lee and others (1983) and summarized in the section "Summary of Previous Application of FESWMS to the Lower Pearl River." Due to cost constraints, only the middle part of the full study reach was considered in the analysis of the four alternative simulations presented in this report. This middle section, approximately 3 mi long and 5 mi wide, is referred to as the study reach or study area The local network or local model discussed in the section "Local-Model Simulation of Seven Alternative Modifications of the I-10 Highway Crossing for the April 2, 1980, Flood" refers to an area 2 0 mi long and 0.7 mi wide, centered along I-10 at the West Pearl River opening All extremes for the period of record referenced in this report are based on data collected through September 1982.

Throughout this report, the words "right" and "left" refer to positions that would be reported by an observer facing downstream The words "backwater" and "drawdown" denote an increase and a decrease, respectively, in water-surface elevation caused by a flood-plain constriction Backwater may occur both upstream and downstream from the constriction Elevations are referenced to the National Geodetic Vertical Datum of 1929 and are called sea level in this report A list of factors for converting inch-pound units to SI units is provided at the end of the report. All data supporting the conclusions of this report are available in the files of the Louisiana District office of the U.S Geological Survey at Baton Rouge, La.

Acknowledgments

The assistance of the following individuals and organizations in making available data for this study is gratefully acknowledged: William T Jack, Jr., and Henry Barrouse, Louisiana Department of Transportation and Development, Office of Highways. The support of the U.S Department of Transportation, Federal Highway Administration, is also gratefully acknowledged

DESCRIPTION OF THE STUDY AREA

Pearl River Basin

The Pearl River basin is approximately 240 mi long and 50 mi wide The basin lies within the Gulf Coastal

Plain and drains a large part of Mississippi and part of southeastern Louisiana The Pearl River originates in Neshoba County, Miss., at the confluence of Nanawaya and Tallahaga Creeks. From its origin, it flows southwestward for 130 mi to the vicinity of Jackson, Miss , then southeastward for another 281 mi to empty into Lake Borgne. Elevations within the basin range from sea level along the coast to about 650 ft above sea level in the north-central hills. The main channel of the Pearl River has a slope of about 1 ft/mi and varies in width from roughly 100 to 1,000 ft. The channel meanders within the flood plain and is obstructed in many places by sand bars, brush, and fallen and overhanging trees The Ross Barnett Reservoir, put into operation in 1961, is just upstream from Jackson, Miss , on the Pearl River and is the only major reservoir within the basin

Most of the low-water flow of the Pearl is transferred to the West Pearl River through Holmes Bayou, 28 mi above the West Mouth of the West Pearl at The Rigolets (fig. 1). Cardwell and others (1967, p. 43) have described this westward shift of flow:

> The bottom lands * * * are laced by cross-connecting channels which distribute flow across these bottoms during periods of high river stage In the vicinity of Picayune, Miss , the main channel of the Pearl River begins to shift westward to become the West Pearl River A small cross channel, Farrs Slough [Farr Slough], leaves the main channel near Picayune and joins Hobolochitto Creek The channel, known downstream as the "Pearl River," begins at this confluence There is evidence that this eastern channel was once the major channel of the lower Pearl River system and that a portion of the old channel near Picayune became filled when the flow shifted to the west * * * It is estimated that during times of minimum flow in the system, less than 5 percent of the flow in the main channel flows through Farrs Slough [Farr Slough] to continue in the eastern channel and the remainder flows through the western channel At maximum flood stages there is considerable flow across the flood plain, and the eastern channel carries the greater part of the flow in the system

From the confluence of Holmes Bayou and the West Pearl River, the main river channels continue generally southward and south-southeastward to the mouths of the Pearl River system The Pearl River flows into Lake Borgne, the West Middle River, a distributary channel, and the East Mouth of the West Pearl River flow into Little Lake; and the West Mouth of the West Pearl River flows into The Rigolets (fig. 1) The drainage area of the Pearl River system is 8,670 mi^2 at the mouths of the system (Shell, 1981, p. 232).

Full Study Reach

The reach of the Pearl River that was studied is in the lower part of the basin along the Mississippi-Louisiana border. As previously mentioned, only the middle part of the full study area, indicated by shading in figure 2, is considered in the analysis presented in this report. The full study reach is located between river miles 9.0 and 26.3 on the Pearl River and river miles 7.9 and 21.9 on the West Pearl River (River miles are defined for each of the channels modeled in detail in this study or in Lee and others (1983) and are shown in figure 2 and on all plates. In each case, zero river mile is defined as the channel mouth.) The full study reach, approximately 12 mi long, is bounded on the north by old U.S. Highway 11 and Interstate Highway 59 and on the south by U.S. Highway 90. The eastern and western boundaries are the natural bluffs at the edge of the flood plain, where ground-surface elevations rise abruptly to 15 to 25 ft above sea level in the northern part of the full study reach and to 5 to 15 ft above sea level in the southern part. Within the full study reach, the axis of the flood plain tends south-southeast, and the flood plain varies in width from about 3 to about 7 mi.

The major channels in the full study reach are the Pearl (known locally as the East Pearl), East Middle, Middle, West Middle, and West Pearl Rivers and Wastehouse Bayou The Pearl flows along the east side of the flood plain, and the West Pearl along the west side. In the northern part of the full study reach, the West Pearl is the largest channel in the flood plain Near Gainesville, Miss., the channel of the Pearl becomes the largest, and it remains the largest to the mouths of the river system.

At river mile 15.2 on the West Pearl River a distributary channel, the Middle River, forms and flows southeastward approximately 3.9 mi, where it divides into the Middle and West Middle Rivers. Approximately 6 3 mi farther south, the Middle River divides again and another distributary channel, the East Middle River, forms South of the full study reach, the East Middle and Middle Rivers flow into the Pearl River about 1.3 mi north of Little Lake. Wastehouse Bayou forms within the flood plain and is tributary to the Pearl River just north of I-10.

There are numerous less significant channels in the flood plain within the full study area. For example, Porters River, a branch of the West Pearl River, forms south of Interstate Highway 59 at river mile 21 4 and rejoins the West Pearl at river mile 17.4. Among the small streams that flow into the Pearl River system in the full study reach are Gum Bayou and Doubloon Branch, which are tributary to the West Pearl River at river miles 14.0 and 10 5, respectively.

Ground-surface elevations of the flood plain range from 1 ft above sea level in the southern part of the full study area to 15 ft above sea level in the northwestern part. Between the upstream boundary and I-10, ground-surface elevations are higher near the West Pearl River than on the east side of the flood plain. Low natural levees border most of the channels in the full study reach. The flood plain has a downstream slope of about 1 ft/mi

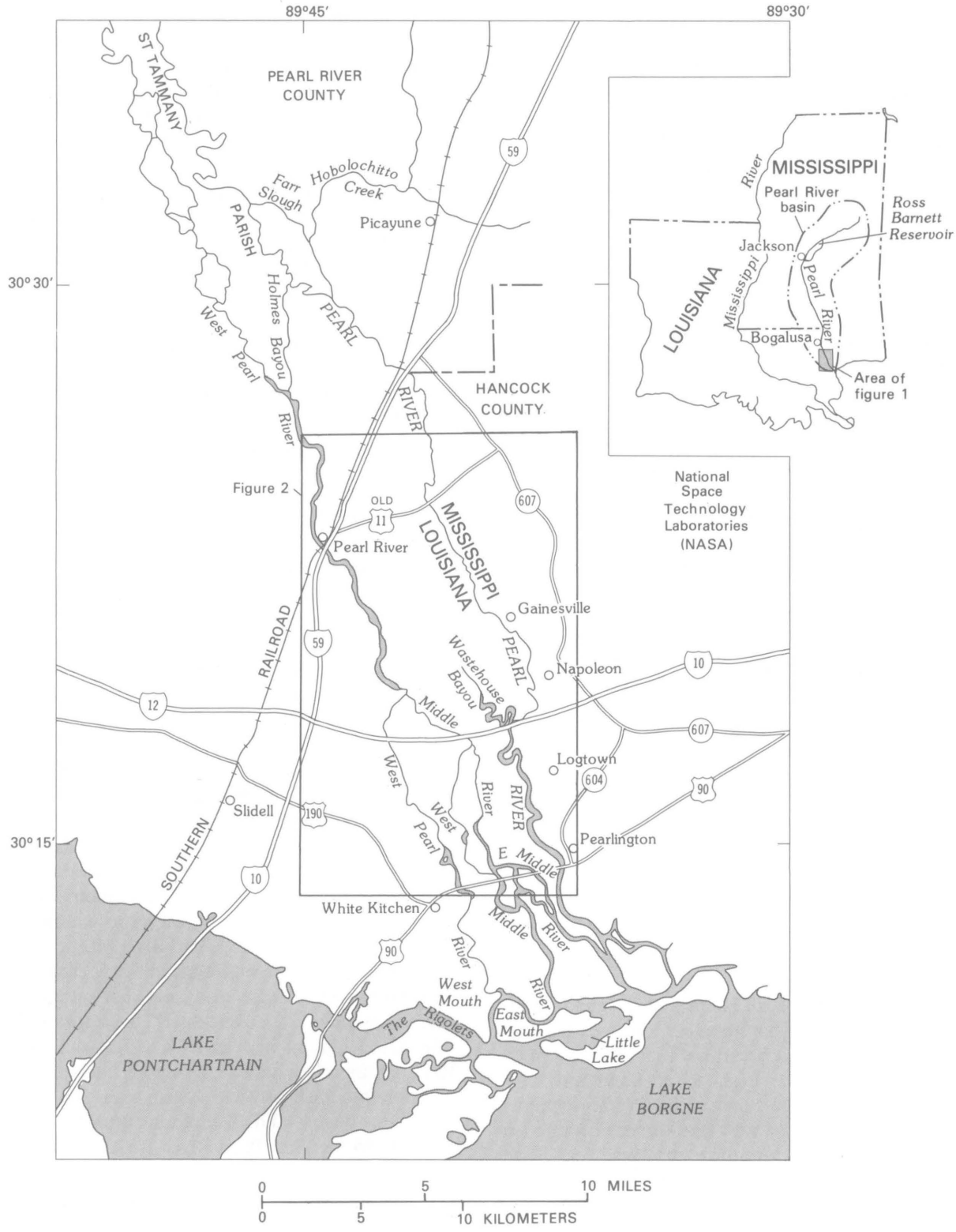

Figure 1. Lower Pearl River basin, Louisiana and Mississippi.

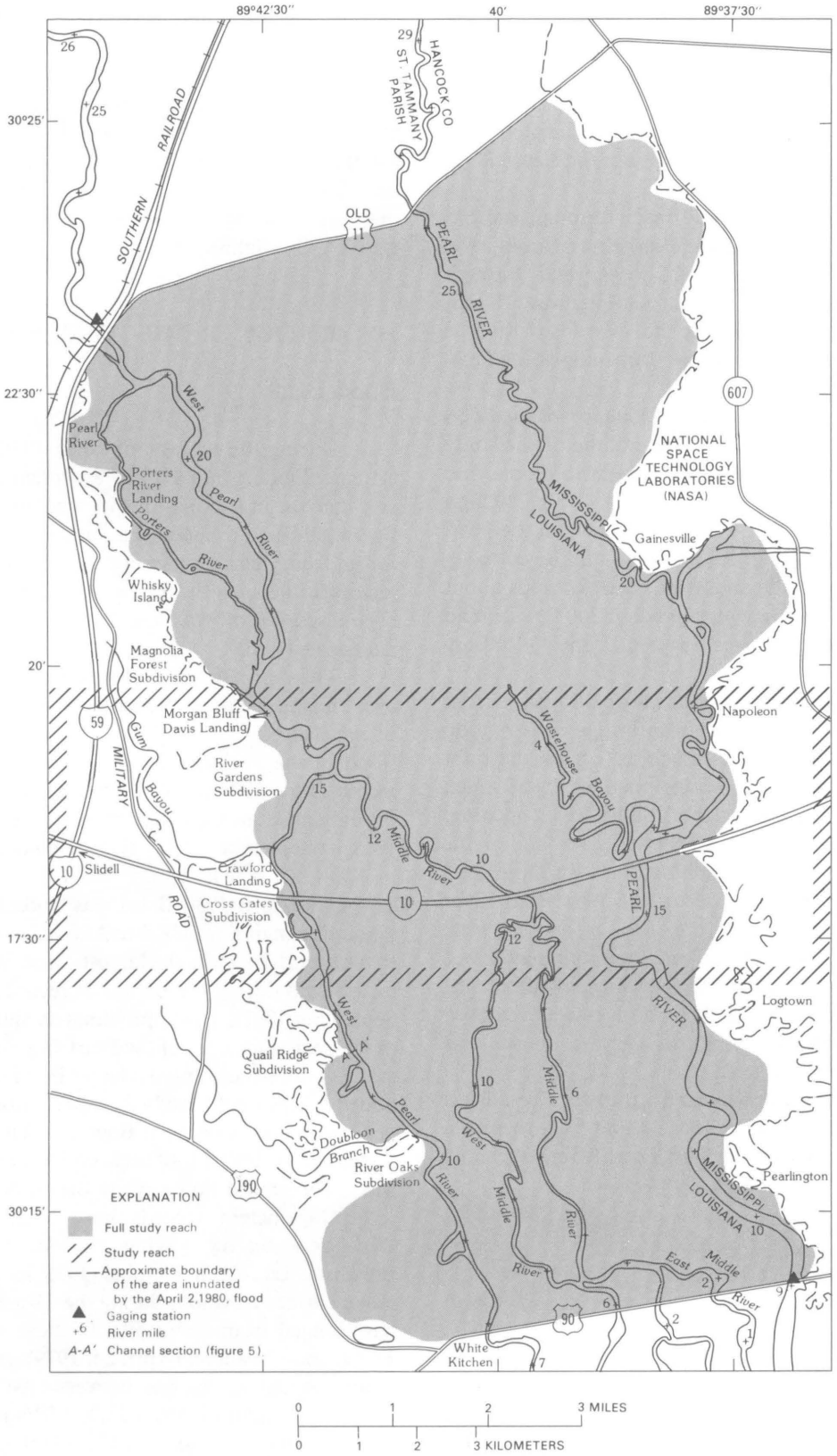

Figure 2. Study reach of the lower Pearl River flood plain near Slidell, La.

The vegetative cover of the study area is shown on plate 1 The flood plain is covered by dense woods, mixed with underbrush in many places The flood-plain forests consist of bottom-land hardwoods and bald cypress-tupelo gum swamps. A small marsh area is located just downstream from the I-10 bridge across the Pearl River at the left edge of the flood plain

Flow enters the full study reach through the old Highway 11 bridge opening at the Pearl River, through the I-59 opening at the West Pearl River, and through numerous small openings in the old Highway 11 embankments. The I-59 opening at the West Pearl River is 2,630 ft wide, and the old Highway 11 opening at the Pearl River is 570 ft wide.

The I-10 crossing, about 4 4 mi long, spans the flood plain in an east-west direction in the middle of the study reach There are bridge openings at the Pearl, Middle, and West Pearl Rivers (fig 3), with widths of 4,980, 770, and 2,240 ft, respectively. The embankment between the Pearl and Middle Rivers is about 0.8 mi long, and the embankment between the Middle and West Pearl Rivers is about 2 1 mi long The embankments are about 300 ft wide, and the elevation of the roadway is between 12 and 13 ft above sea level

Natural flood-plain elevations near I-10 range from 1 to 3 ft above sea level Spoil from bridge construction has increased elevations by as much as 3 ft on the right overbank at the Pearl River bridge opening, by as much as 2 ft on both overbanks at the Middle River opening, and by as much as 6 to 7 ft on the left overbank at the West Pearl River opening. In addition, there is a large knoll adjacent to the southeast corner of the West Pearl River bridge that protrudes into the flow-expansion zone downstream from the bridge This knoll apparently was created during construction of the highway embankments. The vegetation beneath the three bridges was removed during construction, but brush of varying density has grown back in the openings.

A short distance downstream from the West Pearl River bridge, between river miles 12.4 and 13.2, there is a relatively shallow reach of the West Pearl River, where the channel was artificially widened by the removal of earth fill during construction of the highway embankments

Flow leaves the full study reach through five openings in the Highway 90 embankments. The opening widths are 960 ft at the Pearl River, 630 ft at the East Middle River, 580 ft at the Middle River, 580 ft at the West Middle River, and 570 ft at the West Pearl River During the 1980 flood, there was a small amount of flow out of the study area across U.S Highway 190.

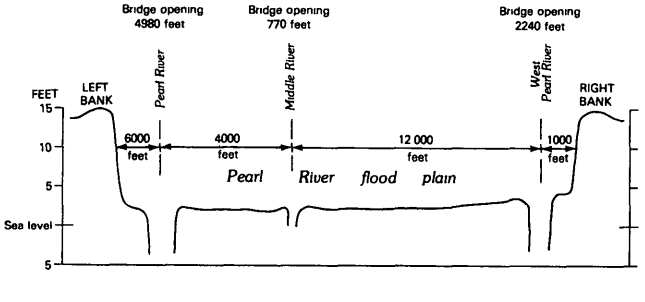

Figure 3. Diagrammatic cross section of flood plain upstream from Interstate Highway 10

HYDROLOGY OF THE PEARL RIVER BASIN

Flood Data

During the months of April 1979 and April 1980, extreme flooding on the Pearl River caused extensive property damage in subdivisions located on the flood plain in the Bogalusa and Slidell, La , areas Many residents were forced from their homes until the floodwater receded. The factors influencing the magnitude of these two events have been discussed by Wax and Tingle (1980) and by Lee and Arcement (1981).

The April 1979 flood was caused by heavy rainfall over the upper part of the basin, where as much as 19 6 in. of rain fell during one 2-day storm This was the largest flood in the Jackson, Miss., area during the period of record (June 1901 to September 1982) and the largest in the Bogalusa area during the period of record (October 1938 to September 1982) (U.S Geological Survey, 1981, p 147; 1983, p. 23)

The April 1980 flood was caused by precipitation amounts ranging from 8.6 to 15 0 in over the entire Pearl River basin. This was the largest flood at Pearl River, La , near Slidell during the period of record (October 1899 to September 1982). The approximately simultaneous arrival of the peak discharges of the Pearl and Bogue Chitto Rivers at their confluence caused a larger flood peak to occur near Slidell than would have been expected on the basis of the peak discharge recorded at Bogalusa. The April 1980 flood forced the closing of I-10 between Slidell and Bay St Louis, Miss., for several hours while the flood crest passed

Gage-height records have been collected at the Geological Survey gaging station, Pearl River near Bogalusa, La , from October 1938 to September 1982 Water-surface elevations during the 43-year period of record have ranged from about 59.8 ft above sea level to about 78.2 ft above sea level (April 24, 1979) At Bogalusa, maximum annual discharges between 1947 and 1982 have ranged in magnitude from 13,200 ft^3/s in 1952 to 129,000 ft^3/s in 1979 (April 24). (See U S Geological Survey, 1983, p 23)

Gage-height records have been collected at the Geological Survey gaging station, Pearl River at Pearl River, La. (fig. 2), from October 1899 to September 1982. Water-

surface elevations have ranged from about 1.5 ft above sea level to about 19.7 ft above sea level (from flood mark, April 1, 1980) during the 82-year period of record. A historical maximum of 20 2 ft above sea level occurred in 1874. At Pearl River, maximum annual discharges between 1947 and 1982 have ranged in magnitude from 17,700 ft^3/s in 1952 to 174,000 ft^3/s in 1980 (April 1). (See U.S Geological Survey, 1983, p 43)

Gage-height records have been collected at the Corps of Engineers gaging station, Pearl River at Pearlington, Miss. (fig 2), from December 1961 to September 1982 Water-surface elevations have ranged from about 2 0 ft below sea level to about 8 4 ft above sea level (September 10, 1965) during the 20-year period of record (U.S Army Corp of Engineers, written commun , 1982) The maximum water-surface elevation during the April 2, 1980, flood was 5.3 ft above sea level.

During the 1961, 1979, and 1980 floods, discharge measurements were made at or near peak flow at various highway crossings in the full study reach. Each of these discharge measurements and the date on which it was made are given in table 1

Approximately 200 high-water marks within and near the full study area were located and flagged by the Geological Survey as the April 1980 floodwater receded. These high-water marks were referenced to sea level and were used by Lee and others (1983) to calibrate their full-reach model

Flood Frequency

After the 1980 flood, the Geological Survey and the Corps of Engineers carried out a coordinated flood-frequency analysis for eight gaging stations on the Pearl River (U.S Geological Survey, written commun., 1980) Discharges for specified recurrence intervals at two of these stations, Bogalusa and Pearl River, are given in table 2, which was taken from Lee and Arcement (1981, p. 35). The values in the table were developed using procedures described by the U.S. Water Resources Council (1977). Skew values and historical flood data used in the analysis were mutually agreed upon by the two agencies. The discharge of 174,000 ft^3/s measured at I-10 on April 2, 1980, is about 3 percent greater than the 50-year discharge at Pearl River

MODEL DESCRIPTION

The core of the modeling system, FESWMS, is a two-dimensional finite-element surface-water flow model based on the work of Norton and King (Norton and King, 1973; Norton and others, 1973, Tseng, 1975, King and Norton, 1978) Around this core, the Geological Survey has

Table 1. Discharges measured during floods on the lower Pearl River in 1961, 1979, and 1980

	Discharge, in cubic feet per second								
	Interstate Highway 59 bridge openings[1]								
Date	1 (Pearl River)	2	3	4	5	6	7	8 (West Pearl River)	Total
Apr 24, 1979	14,800	2,790	5,510	9,110	4,270	5,140	9,620	91,000	142,000
26, 1979	17,700	3,640	7,360	11,200	5,420	5,800	11,600	92,000	155,000

	Interstate Highway 10 bridge openings			
Date	Pearl River	Middle River	West Pearl River	Total
Feb 27, 1961	----------	----------	--------	[2] 106,000
Apr 26, 1979	88,600	29,000	33,800	151,000
May 1, 1979	55,000	16,600	18,700	90,000
Apr 2, 1980	103,000	30,000	40,800	174,000

	Highway 90 bridge openings					
Date	Pearl River	East Middle River	Middle River	West Middle River	West Pearl River	Total
Apr 22, 1980	51,900	11,800	16,700	16,600	6,830	104,000

[1]The bridge openings are numbered from left to right as an observer faces downstream

[2]This measurement was made prior to the construction of Interstate Highway 10

Table 2. Flood-frequency data for the Pearl River at Bogalusa and Pearl River

[These values were mutually agreed upon by the US Geological Survey and the US Army Corps of Engineers]

Station name	Drainage area, in square miles	Discharge, in cubic feet per second, for indicated recurrence interval, in years							
		2	5	10	25	50	100	200	500
Bogalusa----------	6,630	42,500	62,600	77,200	97,000	113,000	129,000	147,000	172,000
Pearl River----------	8,590	56,500	87,000	111,000	143,000	169,000	198,000	228,000	272,000

developed preprocessing and postprocessing programs that make the system more usable. Preprocessing programs place input data in an appropriate form for the flow model and also plot maps of finite-element networks and associated data. Postprocessing programs plot maps of velocity vectors, water-surface contour lines, equal backwater and drawdown lines, discharge at specified cross sections, and observed high-water marks.

The formulation and development of the flow model have been described elsewhere; therefore, only the equations solved and a brief outline of the technique used to solve them are presented here.

Flow Equations

Under the usual assumptions (for example, hydrostatic pressure and momentum correction factors of unity), two-dimensional surface-water flow in the horizontal plane is described by three nonlinear partial-differential equations, two for conservation of momentum and one for conservation of mass (Pritchard, 1971):

$$\frac{\delta u}{\delta t} + u\frac{\delta u}{\delta x} + v\frac{\delta u}{\delta y} + g\frac{\delta h}{\delta x} + g\frac{\delta z_o}{\delta x} - \frac{1}{\varrho h}\left[\frac{\delta}{\delta x}\left(\varepsilon_{xx} h\frac{\delta u}{\delta x}\right) + \frac{\delta}{\delta y}\left(\varepsilon_{xy} h\frac{\delta u}{\delta y}\right)\right] - 2\omega v \sin\phi + \frac{gu}{C^2 h}(u^2+v^2)^{1/2} - \frac{\zeta}{h}V_a^2\cos\psi = 0, \quad (1)$$

$$\frac{\delta v}{\delta t} + u\frac{\delta v}{\delta x} + v\frac{\delta v}{\delta y} + g\frac{\delta h}{\delta y} + g\frac{\delta z_o}{\delta y} - \frac{1}{\varrho h}\left[\frac{\delta}{\delta x}\left(\varepsilon_{yx} h\frac{\delta v}{\delta x}\right) + \frac{\delta}{\delta y}\left(\varepsilon_{yy} h\frac{\delta v}{\delta y}\right)\right] + 2\omega u \sin\phi + \frac{gv}{C^2 h}(u^2+v^2)^{1/2} - \frac{\zeta}{h}V_a^2\sin\psi = 0, \quad (2)$$

and

$$\frac{\delta h}{\delta t} + \frac{\delta}{\delta x}(uh) + \frac{\delta}{\delta y}(vh) = 0, \quad (3)$$

where

C = Chézy coefficient (feet to the one-half power per second),
g = gravitational acceleration (feet per second squared),
h = depth (feet),
t = time (seconds),
u,v = depth-averaged velocity components in the x and y directions, respectively (feet per second),
x,y = Cartesian coordinates in the positive east and north directions, respectively (feet),
V_a = local wind velocity (feet per second),
z_o = bed elevation (feet),
$\varepsilon_{xx},\varepsilon_{xy},\varepsilon_{yx},\varepsilon_{yy}$ = eddy viscosities (pound second per square foot),
ζ = water-surface resistance coefficient (nondimensional),
ϱ = density of water (assumed constant) (slugs per cubic foot),
ϕ = latitude (degrees),
ψ = angle between the wind direction and the x axis (degrees), and
ω = rate of the Earth's angular rotation (per second).

The two-dimensional surface-water flow equations account for energy losses through two mechanisms: bottom friction and turbulent stresses. The Chézy equation for bottom friction in open-channel flow is extended to two dimensions for use in equations 1 and 2. Equations 1 and 2 also use Boussinesq's eddy-viscosity concept, which assumes the turbulent stresses to be proportional to the mean-velocity gradients.

Boundary conditions consist of the specification of flow components or water-surface elevations at open boundaries and zero flow components or zero normal flow (tangential flow) at all other boundaries, called lateral boundaries. For a time-dependent problem, initial condi-

tions must also be specified. Equations 1 through 3, together with properly specified boundary and initial conditions, make up a well-posed initial-boundary-value problem.

Numerical Solution of the Flow Equations

Quadratic basis functions are used to interpolate velocity components, and linear basis functions are used to interpolate depth on triangular, six-node, isoparametric elements (mixed interpolation). Model topography is defined by assigning a ground-surface elevation to each element vertex and requiring the ground surface to vary linearly within an element.

The finite-element model requires the specification of a constant Chézy coefficient, C, and a constant symmetric turbulent-exchange, or eddy-viscosity, tensor, ε, over each element. Nonisotropic turbulent stresses can be simulated by assigning different values to the components of the eddy-viscosity tensor. The eddy-viscosity terms in the momentum equations suppress nonlinear instabilities generated by the convective terms, and nonzero eddy-viscosity values are necessary for convergence of the numerical method to a solution. The eddy-viscosity values can influence the results of a simulation; however, optimum values are difficult to determine. In general, increased values serve to increase water-surface slopes. It is also known that eddy-viscosity values should increase with element size.

Flow components are specified at inflow boundary nodes, and water-surface elevations are specified at outflow boundary nodes. In this study, zero normal flow (tangential flow) was specified at all lateral boundaries. Isoparametric elements permit the use of smooth, curved lateral boundaries. The improvement in accuracy obtained by using such boundaries, together with the specification of zero normal flow at the boundaries, has been documented by Gee and MacArthur (1978), King and Norton (1978), and Walters and Cheng (1978, 1980) for the mixed-interpolation formulation of the surface-water flow equations

Galerkin's method of weighted residuals, a Newton-Raphson iteration scheme, numerical integration using seven-point Gaussian quadrature (Zienkiewicz, 1977, p 200–201), and a frontal solution algorithm using out-of-core storage (Hood, 1976, 1977) are used to solve for the nodal values of the velocity components and depth. The time derivatives are handled by an implicit finite-difference scheme; in the application reported here, however, only the steady-state forms of the equations were solved.

If a finite-element network is not well designed, errors in conservation of mass can be significant because there are only approximately half as many equations for conservation of momentum in either the x or the y direction For a well-designed network, however, errors in mass conservation are small. The model has the capability of integrating the discharge across a line (called a continuity-check line) following element sides and beginning and ending at element vertices Thus, conservation of mass can be checked (King and Norton, 1978).

Gee and MacArthur (1982) completed a cursory study of continuity-check errors with a two-dimensional finite-element model similar to the one used in this study. They concluded that the solution is acceptable if the discharge at all continuity-check lines does not deviate from the input discharge by more than ± 5 percent.

The interested reader may consult books by Pinder and Gray (1977) and Zienkiewicz (1977) for additional information on the finite-element method.

SUMMARY OF PREVIOUS APPLICATION OF FESWMS TO THE LOWER PEARL RIVER

Lee and others (1983) used the two-dimensional finite-element surface-water flow-modeling system, FESWMS, to determine the effect of I-10 on Pearl River flooding during the April 2, 1980, flood. The results of their work are summarized in this section. The procedure used in their study follows. Hydrographic and topographic data were collected and were used to define the region to be modeled, to design an equivalent finite-element network that included the I-10 embankments, to establish model boundary conditions, to verify that a steady-state model analysis is valid, and to calibrate the flow model by simulating the April 1980 flood as closely as possible. Next, the finite-element network was modified to represent conditions without I-10 in place Finally, the hydraulic effect of I-10 was determined by comparing model results with and without I-10.

Simulation of the April 2, 1980, Flood with the Interstate Highway 10 Embankments in Place

Data Collection and Analysis

A large amount of hydrographic and topographic data was collected and analyzed for use in modeling the April 1980 flood Gage-height records collected at Pearl River, La , at the upper end of the full study reach, and at Pearlington, Miss , at the lower end of the reach, were used to verify the steady-state assumption. At the time of the downstream peak, the upstream water-surface elevation had fallen less than 0.5 ft from its maximum value. On the basis of this observation, it was assumed for modeling purposes that the flow was steady. The steady-state

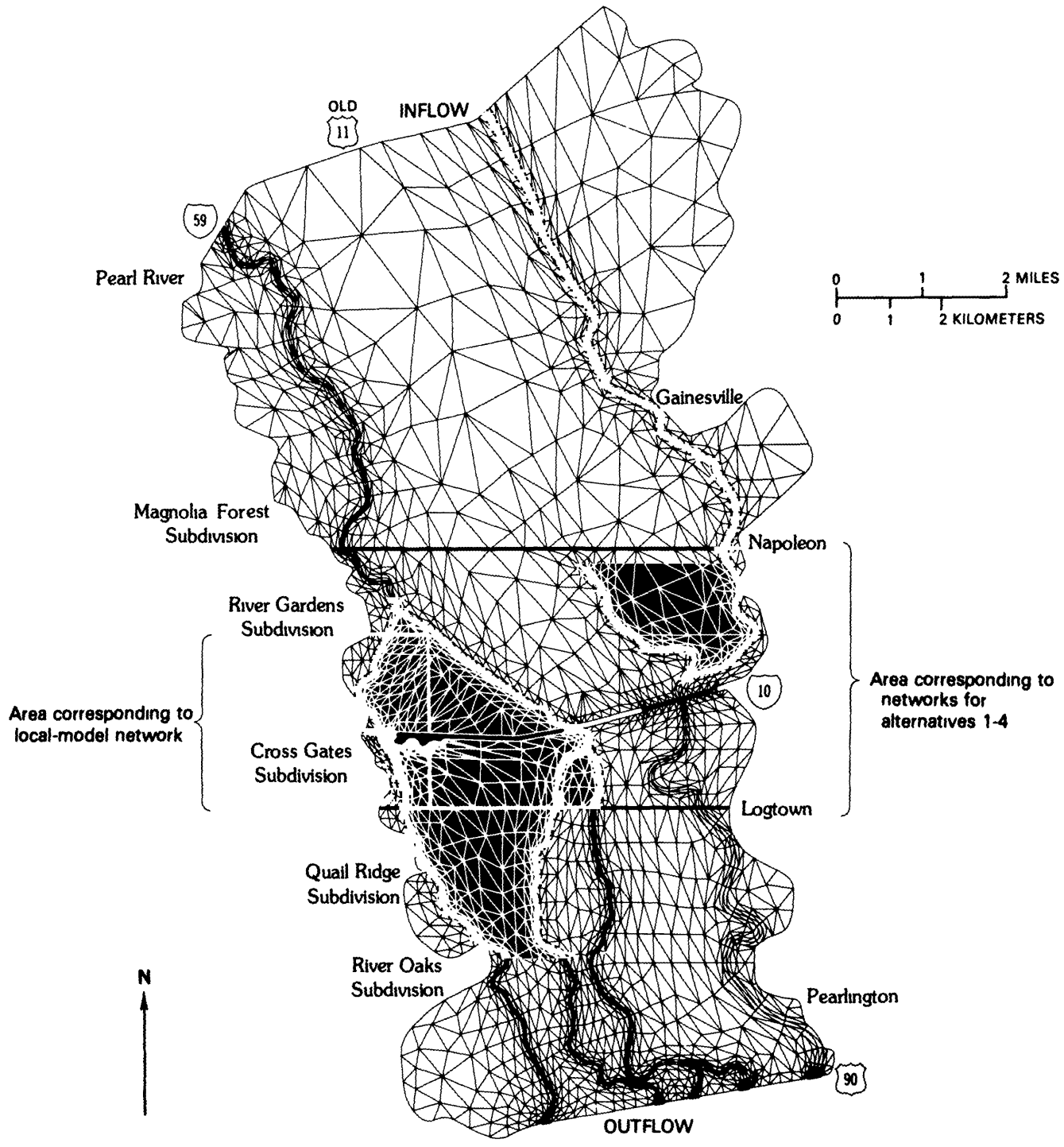

Figure 4. Finite-element network for the full study reach simulation

discharge, required as input at the upstream boundary in the model, was obtained from a discharge measurement made by the Geological Survey at I-10

Approximately 50 mi of longitudinal channel profiles were obtained for the significant channels in the full study reach. Also, 73 representative and special-purpose cross-section surveys were made to define channel geometry. Detailed topographic data at and near bridge openings were obtained from the Office of Highways.

Infrared aerial photographs of the full study area and field observations were used to determine vegetation type and density. The collected data were supplemented by historic hydrologic data and Geological Survey topographic maps.

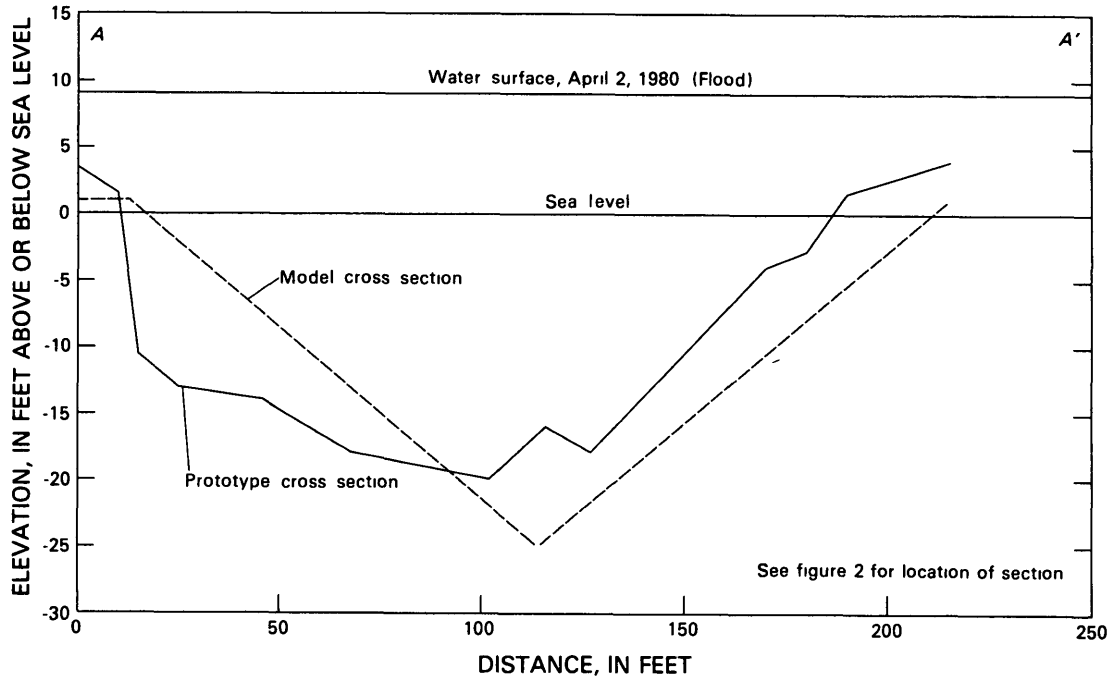

Figure 5. Prototype and model cross sections of channel at section *A–A'*

Network Design

The network, shown in figure 4, was designed to represent closely the highly nonuniform boundary of the area inundated by the April 1980 flood The upstream boundary was located parallel to old Highway 11 and I-59, where inflows could be distributed on the basis of earlier discharge measurements. The downstream model boundary was located parallel to Highway 90, and outflows were placed at the five bridge openings, where water-surface elevations could be estimated on the basis of nearby high-water marks. Modifications to the existing I-10 embankments were assumed to have little effect on the boundary conditions, because both the upstream and downstream boundaries were at least one flood-plain width distant from the highway crossing.

After the boundaries were defined, the full study area was divided into an equivalent network of triangular elements. Subdivision lines between elements were located where there are abrupt changes in vegetative cover or topography Each element was designed to represent an area of nearly homogeneous vegetative cover. In areas where velocity, depth, and water-surface gradients were expected to be large, such as near bridge openings and in areas between overbanks and channel bottoms, network detail was increased to facilitate better simulation of the large gradients by the flow model.

The use of elements with aspect ratios (the ratio of the longest element side to the shortest) greater than unity made it possible to design the network with fewer elements than would have been required otherwise. Such elements were used primarily in defining river channels The longest element side was aligned with the assumed flow direction; velocity and depth changes would typically be small in this direction. Most element aspect ratios were kept below a maximum of about 10

The complex geometry of the flood plain of the Pearl River was modeled in detail. Most prototype lengths and widths were realistically represented in the model; however, to keep the number of elements in the network at a manageable level, several approximations were made. Only large channels were included in the network. Prototype channel cross sections were represented in the model by either triangular or trapezoidal cross sections, with cross-sectional areas equal to the measured areas (fig 5) Some meandering channel reaches with relatively small flows were replaced with artificially straightened, but hydraulically equivalent, reaches The width of simulated stream channels was kept to a minimum of 200 ft

In its complete state, the finite-element network used by Lee and others (1983) contained 5,224 triangular elements and 10,771 computational nodes. The middle grid used in this study contained 2,000 to 2,200 triangular elements and 4,300 to 4,700 computational nodes, depending on the alternative modification.

Boundary Conditions

The discharge at the upstream boundary (table 3) was the peak discharge of 174,000 ft^3/s measured at I-10 on

Table 3. Distribution of discharge at the upstream model boundary

Section of upstream boundary	Discharge, in cubic feet per second	Discharge, as percent of total discharge
Flood plain between eastern edge of flood plain and Pearl River	22,100	12 7
Pearl River bridge opening	22,000	12 6
Flood plain between Pearl and West Pearl Rivers	32,900	18 9
West Pearl River channel	69,100	39 7
Flood plain between West Pearl River and western edge of flood plain	28,200	16 2
Total	174,000	100 0

April 2, 1980. It was distributed among the inflow boundary nodes on the basis of previous discharge measurements at the bridge openings in old Highway 11 and I-59. Inflow was concentrated at the old Highway 11 bridge across the Pearl River and the I-59 bridge across the West Pearl River. Flow into the study reach through numerous small openings in old Highway 11 was represented as continuous inflow between the east edge of the flood plain and the Pearl River and between the Pearl and West Pearl Rivers. Water-surface elevations at the downstream boundary were determined from high-water marks near the five bridge openings in Highway 90.

Model Calibration

The model-adjustment process consisted of two parts. the adjustment of empirical model coefficients (model calibration) and the adjustment of model boundary conditions, network detail, and ground-surface elevations on the basis of additional information obtained during the study.

On the basis of previous finite-element simulations, the values of all components of the eddy-viscosity tensor were initially set at 100 lb · s/ft^2 for all elements in the network Numerical experiments indicated that once the values of these coefficients were set high enough to ensure convergence, the solution was much less sensitive to changes in their values than to changes in the values of the Chézy coefficients. Because of a lack of information about their correct values and to avoid convergence problems, the values of all components of the eddy-viscosity tensor were maintained at 100 lb · s/ft^2 throughout the study for all elements in the network.

Once the values of eddy viscosity were fixed, preliminary calibration work focused on determining the values of Chézy coefficients Nominal values were selected for initial use with the model on the basis of infrared aerial photographs of the flood plain and field inspection. In making both the initial estimates of the Chézy values and subsequent modifications to them, care was taken to ensure that the assigned values were reasonable and mutually consistent:

A series of simulations was conducted to determine the relative effect on water-surface elevations of changes in the values of the Chézy coefficients of both overbank and channel elements. Computed water-surface elevations were most sensitive to changes in the value of the Chézy coefficient of the wooded flood plain. Changes in the Chézy values of the channel elements had little or no effect on computed water-surface elevations, except for channel reaches carrying a significant percentage of the total flow. Such reaches included the Pearl River between I-10 and Highway 90 and reaches located a few thousand feet upstream and downstream from bridge openings. Computed water-surface elevations were also moderately sensitive to the values of the Chézy coefficients of the overbank areas under the three I-10 bridges

Preliminary calibration consisted of matching as closely as possible all observed high-water marks as well as measured discharges at the three bridge openings in I-10.

Appropriate adjustments to the values of the Chézy coefficients gave close agreement between computed and observed data in most cases. In several areas, however, discrepancies between model results and observations made it necessary to check the location and elevation of a few high-water marks and to study previously overlooked local topographic features. On the basis of the results of the early simulations and the additional observations, modifications were made to model boundary conditions, network detail, and model ground-surface elevations. During this adjustment process, it was observed that computed water-surface elevations along the upstream model boundary were sensitive to changes in the upstream discharge distribution and that the distribution of discharge among the three I-10 bridge openings was affected significantly by flood-plain ground-surface elevations at and near the three I-10 openings.

After these adjustments were completed, minor adjustments to the values of the Chézy coefficients were needed for final calibration of the model. The final Chézy values were 22 ft$^{1/2}$/s for the wooded flood plain, 28 to 35 ft$^{1/2}$/s for the marsh-grass areas, 21 to 40 ft$^{1/2}$/s for the overbank areas under the three I-10 bridges, and 85 to 115 ft$^{1/2}$/s for the unstraightened channels. Computed flow depths ranged from 2 to 23 ft for the wooded flood plain, from 4 to 10 ft for the marsh-grass areas, from 4 to 9 ft for the overbank areas under the I-10 bridges, and from 5 to 47 ft for the unstraightened channels. On the basis of these depths, values of the Manning n corresponding to the final Chézy values range from 0.077 to 0.114 ft$^{1/6}$ for the wooded flood plain, from 0 055 to 0.074 ft$^{1/6}$ for the marsh-grass areas, from 0.046 to 0.098 ft$^{1/6}$ for the overbank areas under the I-10 bridges, and from 0.021 to 0.033 ft$^{1/6}$ for the unstraightened channels.

Computed flow depths averaged about 21 ft in the channels and about 8 ft on the flood plain. Average channel velocities were between 1 and 3 ft/s at most cross sections. Somewhat higher velocities occurred at several of the bridge openings. The average velocity on the flood plain was about 0.7 ft/s.

Comparison of Simulated and Observed Values

The computed water-surface elevation is in close agreement with the elevation of the observed high-water mark or marks at most of the locations where high-water marks were available. The root mean square difference between the computed and observed values is 0.18 ft. The computed water-surface elevations are within ±0.3 ft of the elevations of the high-water marks at all but four locations, and at these four locations, the computed water-surface elevations are within ±0.5 ft of the observed.

The discharge measurement made at the I-10 bridge openings on April 2, 1980, and listed in table 4 was also used in model calibration. The computed discharges given in table 4 were obtained from continuity checks across each opening. The errors in computed discharge at the bridge openings at the Pearl, Middle, and West Pearl Rivers, as a percentage of the measured discharge at each opening, are 7, −10, and −7, respectively. The sum of the computed discharges at the three openings is 175,000 ft^3/s. The cause of the 1,000 ft^3/s difference between the total computed discharge at I-10 and the total upstream inflow is a model limitation discussed in the section "Numerical Solution of the Flow Equations." Because the computed discharge deviates from the input discharge by less than 1 percent, the computed discharge is considered acceptable.

Table 4. Computed and measured discharges at the Interstate Highway 10 bridge openings

Opening section	Discharge, in cubic feet per second	
	Computed	Measured
Pearl River		
Left overbank----	23,600	21,500
Channel----------	50,200	52,000
Right overbank--	36,100	29,600
Total----------	110,000	103,000
Middle River		
Left overbank----	3,810	1,920
Channel----------	17,800	20,400
Right overbank--	5,360	7,670
Total----------	27,000	30,000
West Pearl River		
Left overbank----	10,000	11,300
Channel----------	16,900	19,700
Right overbank--	11,000	9,800
Total----------	37,900	40,800

Unit discharge (defined as discharge per unit distance), both computed and measured, is plotted as a function of distance at each of the three I-10 bridge openings in figures 6, 7, and 8. In general, there is a good agreement between the computed and observed profiles,

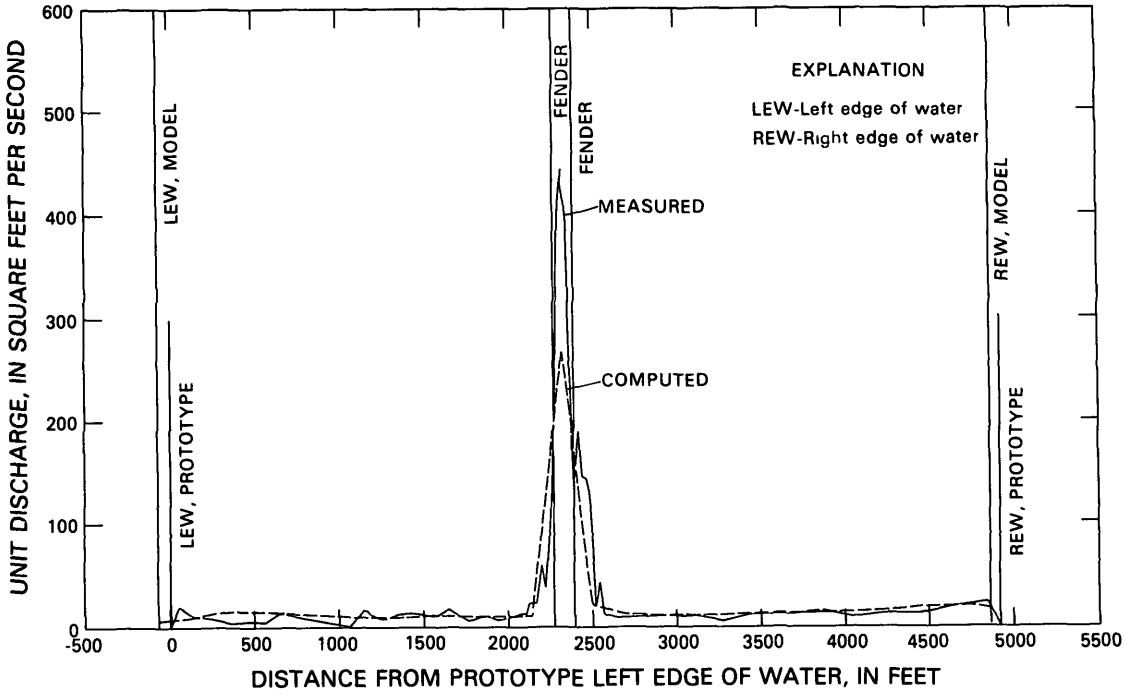

Figure 6. Computed and measured unit discharge at the Interstate Highway 10 bridge opening at the Pearl River

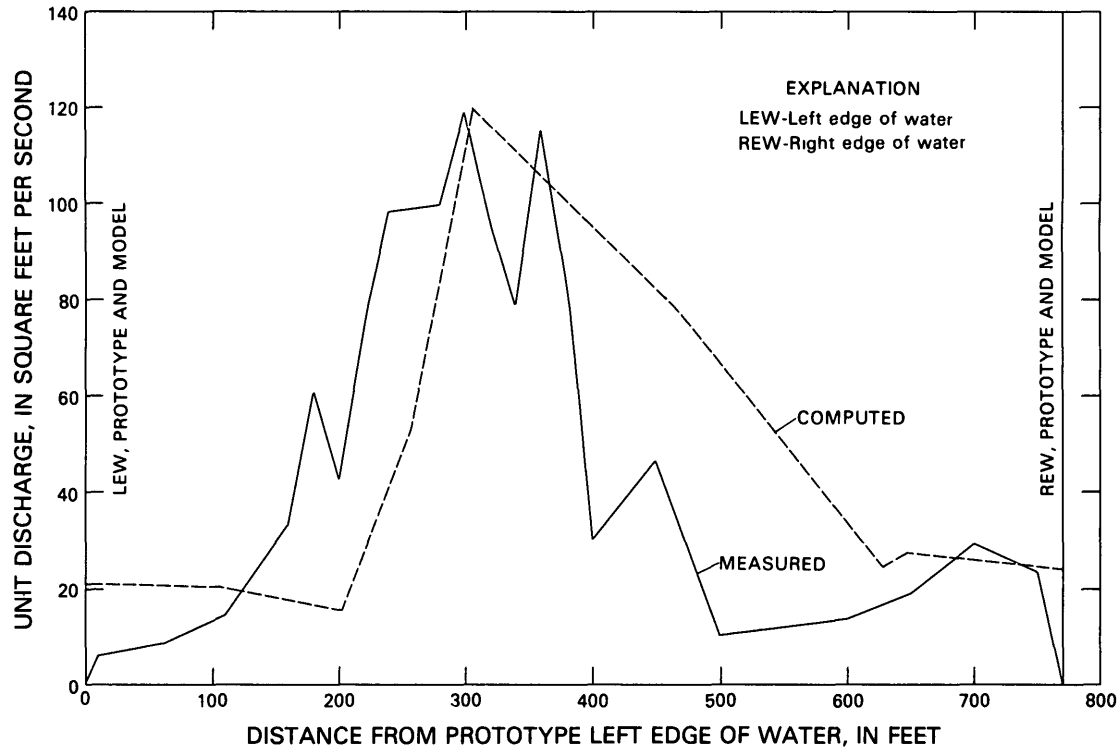

Figure 7. Computed and measured unit discharge at the Interstate Highway 10 bridge opening at the Middle River

especially for the overbank areas. The profiles based on field observations are more variable than the computed profiles because of debris, flow around piers and fenders, and local variations in topography and vegetative cover. Because the main-channel fenders at the Pearl and West Pearl Rivers were not modeled in the study of Lee and others (1983) or in this study, the peak unit discharges at the openings are underestimated by the model.

Analysis of the calibration simulation provides some additional information related to discharge distribution and to the direction of the flow field within the full study area. Between the upstream boundary and I-10, there is a movement of water from the west to the east side of the flood plain. At the upstream boundary, 56 percent of the inflow passed through the bridge opening at the West Pearl River, but at I-10, 59 percent of the measured discharge passed through the bridge opening at the Pearl River. The model accurately simulated the observed shift, as 63 percent of the computed discharge passes through the Pearl River bridge opening at I-10 As expected, the velocity field in this reach is aligned in a generally southeastward direction.

The water-surface contours for the calibration simulation are shown in figure 9. The 15.5- to 20.5-ft water-surface contours indicate a "mound" downstream from the I-59 bridge opening at the West Pearl River. Between 3 and 4 mi downstream, the alignment and spacing of the contour lines indicate that the flow has become uniformly distributed across the flood plain. Then, within a 3-mile-long reach centered about I-10, the flow converges toward and passes through the three bridge openings and then diverges back onto the flood plain. Approximately 1.5 mi downstream from the highway crossing, the flow is again uniformly distributed across the flood plain, as indicated by the water-surface contours shown in figure 9.

Simulation of the April 2, 1980, Flood Without the Interstate Highway 10 Embankments in Place

The finite-element network used to simulate the April 1980 flood was modified to represent conditions without I-10 in place, and the hydraulic impact of the I-10 embankments was determined by comparing computed results with and without I-10.

It should be noted that conditions with I-10 were compared with conditions without I-10, not with conditions prior to the construction of I-10. Thus, the reach of the West Pearl River between river miles 12.4 and 13 2, which was widened during construction, was not restored

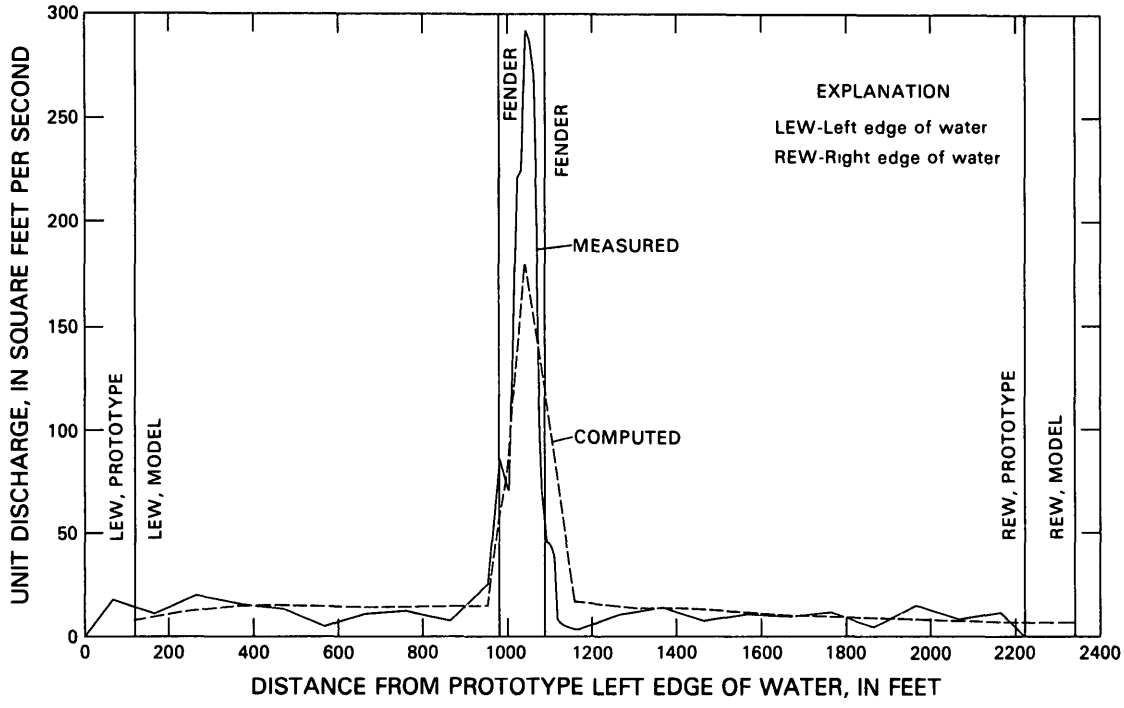

Figure 8. Computed and measured unit discharge at the Interstate Highway 10 bridge opening at the West Pearl River

to its original width and depth in the simulation without I-10. However, because of the relatively small flow in the channel of the West Pearl River without I-10 in place, the difference with respect to backwater between conditions without I-10 and conditions prior to the construction of I-10 is almost certainly negligible.

Network Modifications

Elements were added in the areas occupied in the original network by the I-10 embankments Elsewhere, the two networks were identical. Model ground-surface elevations at and near the highway embankments were changed to the elevation of the surrounding natural flood plain. The Chézy coefficients corresponding to the new elements and the elements formerly located in overbank areas under the I-10 bridges were assigned the value 22 $ft^{1/2}/s$, the value used in both simulations for the wooded flood plain. Upstream and downstream boundary conditions were the same as those used in the simulation with the highway embankments in place.

Results of the Simulation

The water-surface contours for the simulation without I-10 in place are shown in figure 10. Water-surface elevations upstream from the I-10 site are lower without the highway embankments in place. Flow patterns in the upper and lower parts of the full study reach are similar to those computed with the highway embankments in place. Throughout the middle part of the study reach, the flow is uniformly distributed across the flood plain and is parallel to the flood-plain axis Without I-10 in place, the flow shift from the west side of the flood plain to the east side does not occur as far upstream as with I-10 in place.

Computed discharges at the site of I-10 with and without the highway embankments in place are given in table 5. Without the highway embankments in place, flow is reduced 41 percent at the Pearl River bridge opening, 80 percent at the Middle River opening, and 67 percent at the West Pearl River opening. Without the roadway in place, the computed discharge across that part of the flood plain that is occupied by the embankments with the roadway present is 95,200 ft^3/s.

Backwater and Drawdown Caused by the Interstate Highway 10 Embankments

A map of backwater and drawdown was obtained by subtracting nodal water-surface elevations computed without the roadway in place from the corresponding nodal water-surface elevations computed with the roadway

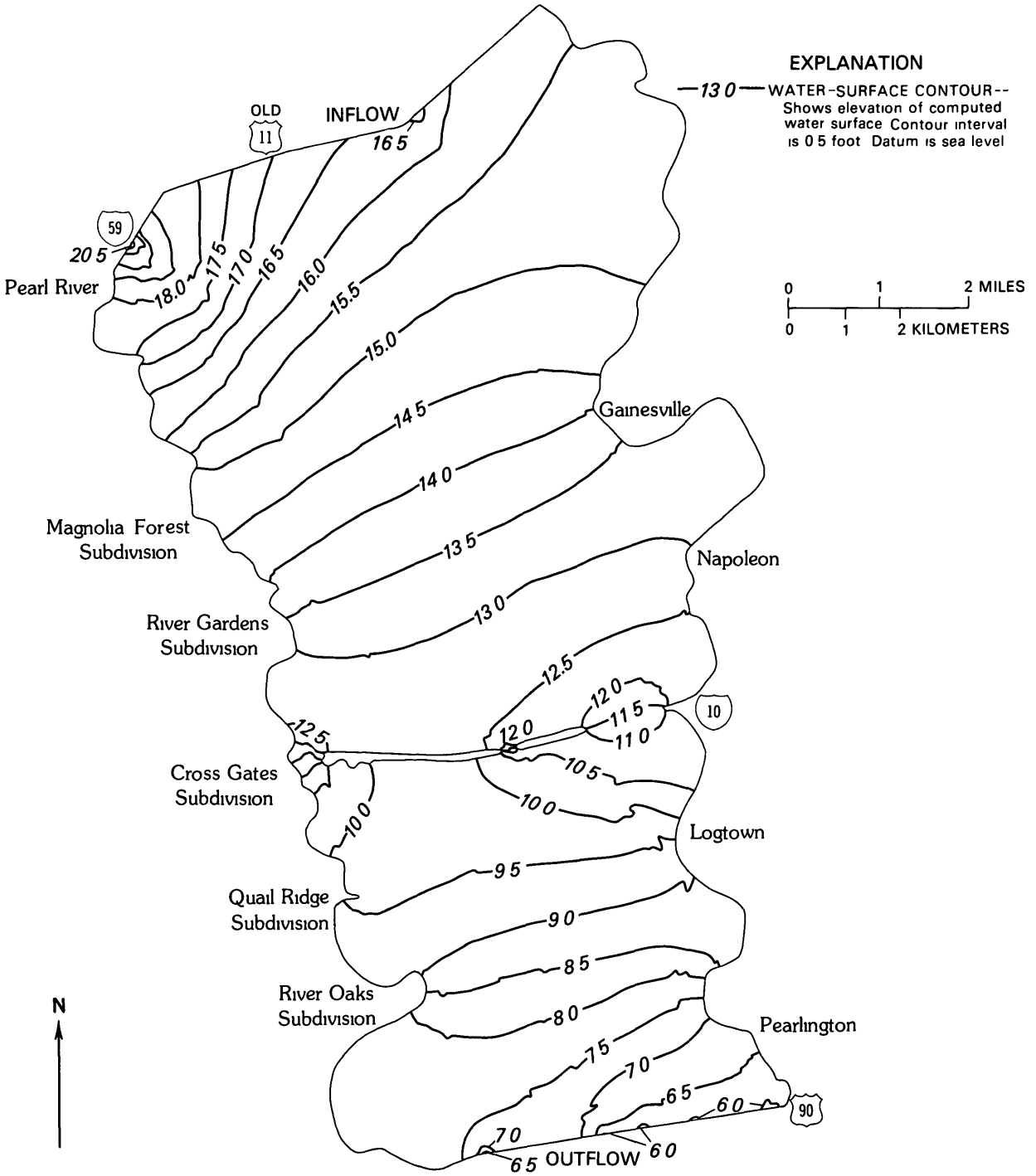

Figure 9. Computed water-surface contours for the full study reach with the Interstate Highway 10 embankments in place

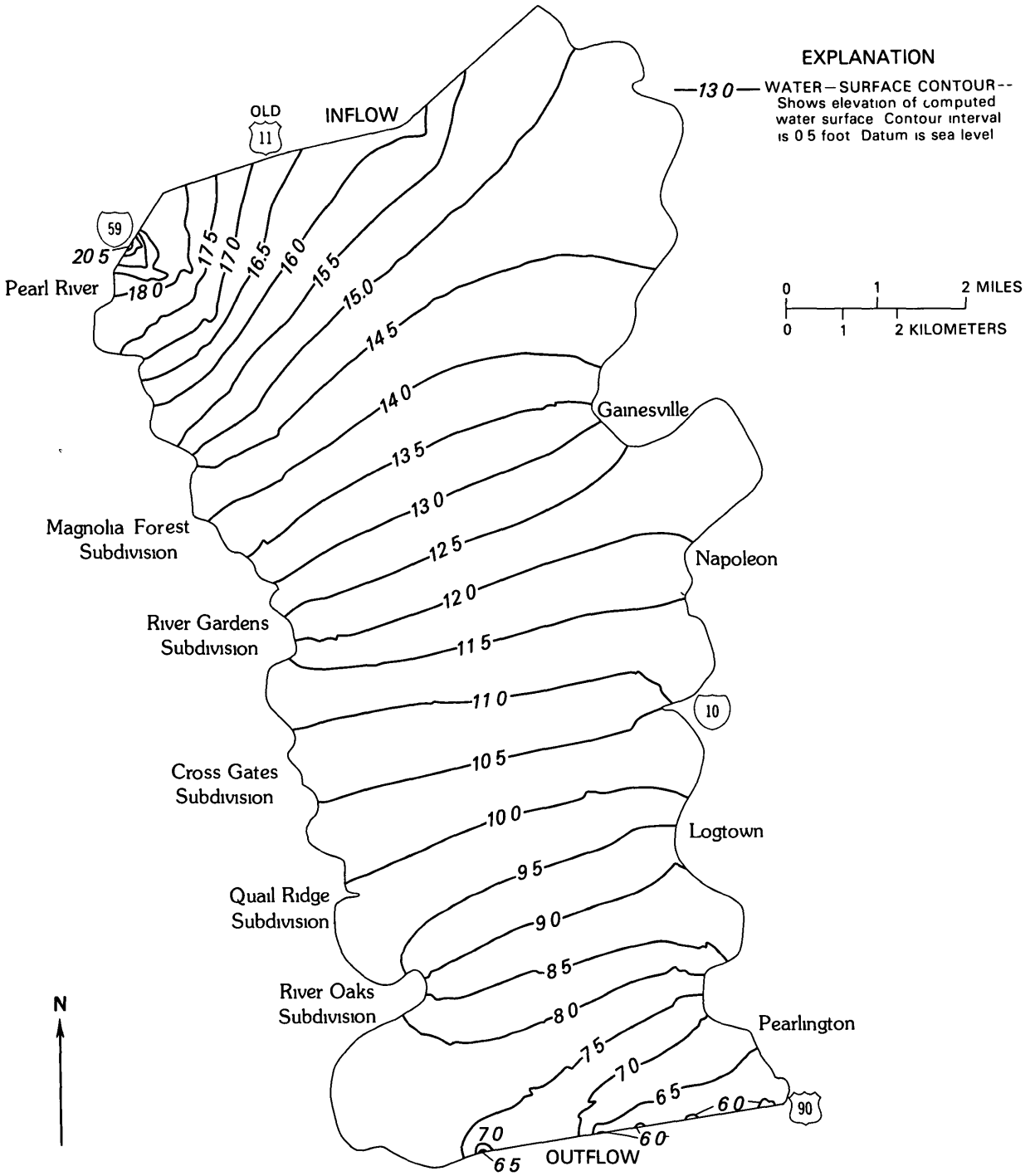

Figure 10. Computed water-surface contours for the full study reach with the Interstate Highway 10 embankments removed

Table 5. Computed discharges at Interstate Highway 10 with and without the embankments

Subsection	Discharge, in cubic feet per second: With highway embankments	Without highway embankments
Embankment between left edge of flood plain and Pearl River	0	833
Pearl River, left overbank	23,600	13,800
Pearl River, channel	50,200	32,500
Pearl River, right overbank	36,100	18,100
Pearl River, total	110,000	64,400
Embankment between Pearl and Middle Rivers	0	29,900
Middle River, left overbank	3,810	916
Middle River, channel	17,800	3,320
Middle River, right overbank	5,360	1,100
Middle River, total	27,000	5,340
Embankment between Middle and West Pearl Rivers	0	64,500
West Pearl River, left overbank	10,000	3,560
West Pearl River, channel	16,900	5,260
West Pearl River, right overbank	11,000	3,580
West Pearl River, total	37,900	12,400
Total[1]	175,000	177,000

[1]The reason for the discrepancy among the total computed discharges and the total inflow is discussed in the section, "Numerical Solution of the Flow Equations "

in place. Lines of equal backwater and drawdown are shown in figure 11. The 1.2-ft to 2.0-ft lines form a "mound" north of I-10 between the right abutment of the Pearl River bridge and the west edge of the flood plain. Upstream from the roadway, maximum backwater at the west edge of the flood plain (1.5 ft) is greater than maximum backwater at the east edge (1.1 ft), but backwater decreases more rapidly in the upstream direction along the west edge than along the east edge.

Backwater ranging from 0.6 to 0.2 ft extends more than a mile downstream from the Pearl River bridge opening in I-10 at the east edge of the flood plain. A large area of drawdown extends from the downstream side of the highway embankment between the Middle and West Pearl Rivers to the west edge of the flood plain. The lateral variations in backwater and drawdown are due to the relatively greater constriction of the flow in the western part of the flood plain and to the topography of the flood plain.

LOCAL-MODEL SIMULATION OF SEVEN ALTERNATIVE MODIFICATIONS OF THE INTERSTATE HIGHWAY 10 CROSSING FOR THE APRIL 2, 1980, FLOOD

A local model was developed to determine the probable effects of several flood-plain and structural modifications of the I-10 crossing. The modifications consist of three alternatives involving clearing of vegetation, three alternatives requiring removal of spoil, and one alternative simulating the installation of culverts in the I-10 embankment. The local model is less costly to use than either the large model used in the full study reach or the model used to analyze the four alternative modifications discussed in the next section.

In the present study, local-model simulations were used to aid in selecting the four alternatives to be simulated by the larger model presented in the next section of this report. A note of caution is warranted, because results obtained from an alternative simulation using the local model will differ somewhat from results obtained from the same alternative simulation using either the full-reach network shown in figure 4 or the networks shown in figures 13, 20, and 29. This difference in computed results occurs because the fixed-boundary conditions are in close proximity to the areas modified; thus, they will influence the solution.

Network Design, Boundary Conditions, and Validation

The local network, shown in figure 12, was designed to represent the area near the West Pearl River opening inundated by the April 1980 flood. The local-model network differs slightly from the corresponding section of the full-reach network (fig. 4). Prototype channel widths were more closely approximated by the channel widths in the local network than by those in the full-reach network, but the cross-sectional areas of the channels in both networks are equal to the measured cross-sectional areas of the prototype. Ground-surface elevations, embankment geometry, and Chézy values were selected to match, as closely as possible, the values used in the full-reach model discussed in the previous section.

The boundary conditions for the local model were taken from the results of the full-reach calibration simulation at the closest corresponding nodes. The local-model inflow along the upstream boundary and the eastern boundary north of I-10 was adjusted in direction and magnitude to match the results from the full-reach calibration simulation (table 6). Water-surface elevations were set along the downstream boundary and the eastern boundary south of I-10.

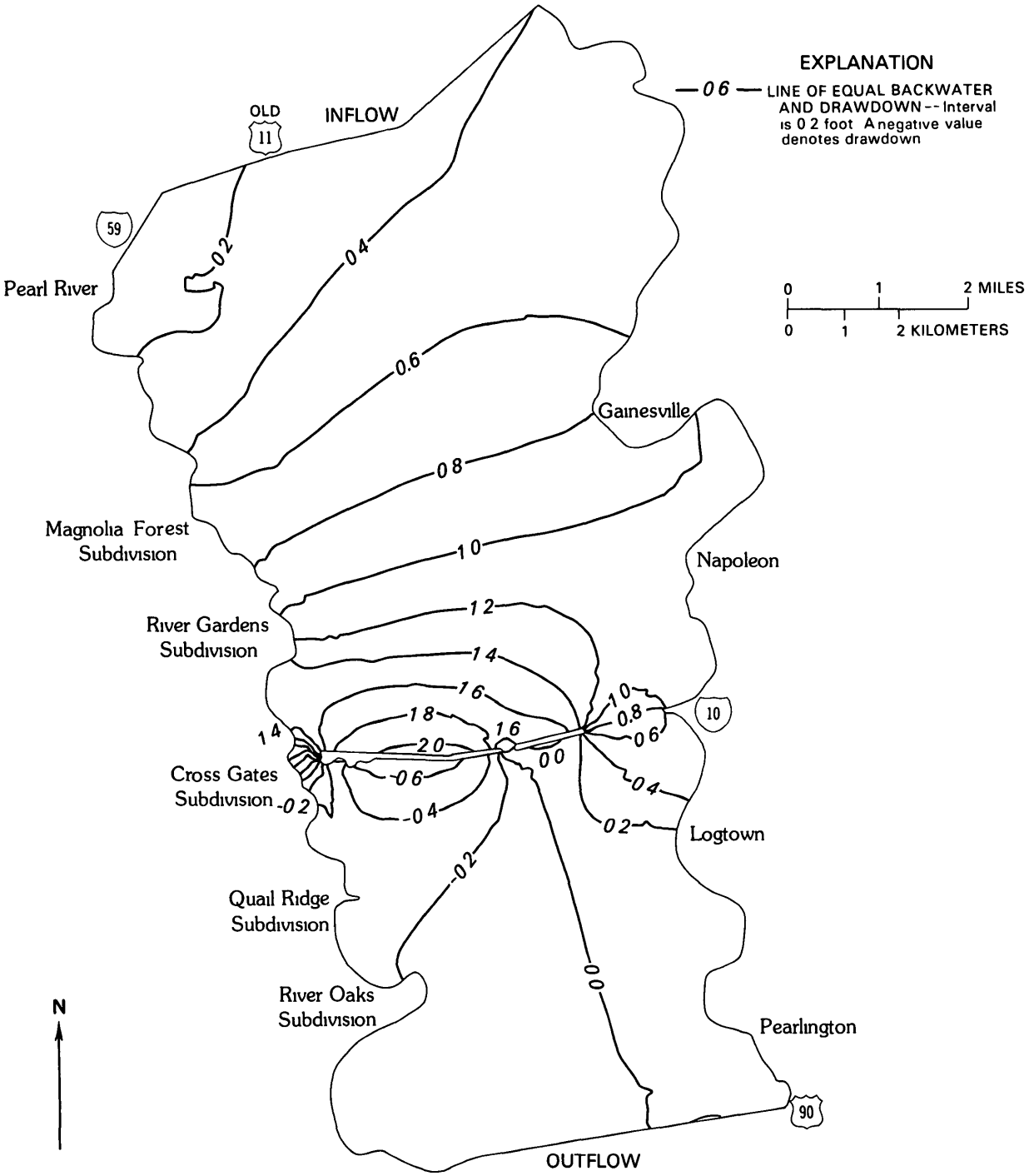

Figure 11. Line of equal backwater and drawdown with Interstate Highway 10 in place for the April 2, 1980, flood

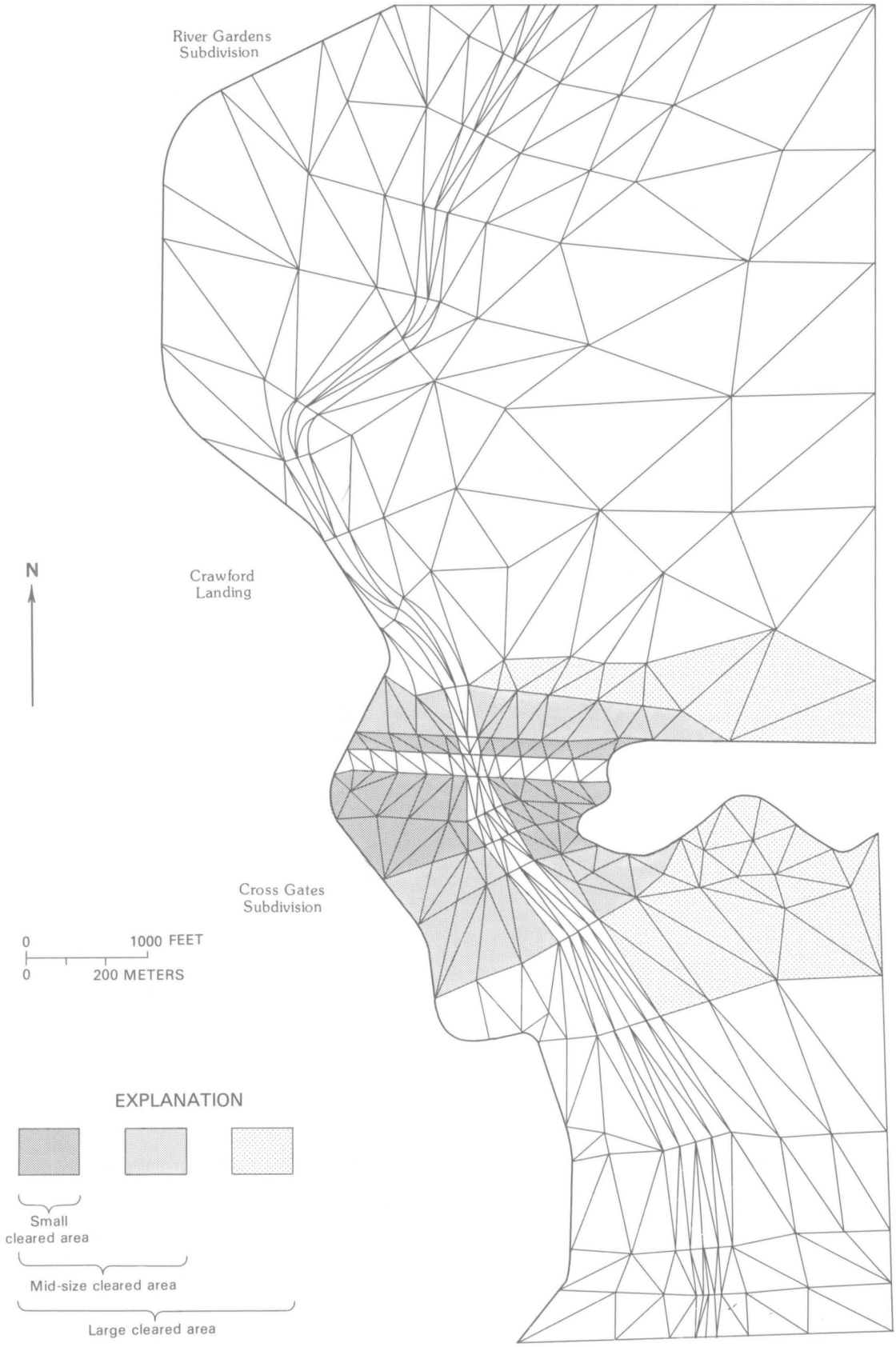

Figure 12. Finite-element network for the local-model simulations.

Table 6. Discharges along the upstream boundary of the local model computed using the full-reach model and input discharges along the upstream boundary of the local model

Section of upstream boundary	Discharge, in cubic feet per second	
	Full-reach model	Local model
Right overbank	8,220	8,340
Main channel	6,230	5,830
Left overbank	14,700	14,400
Eastern boundary	8,860	9,350
Total	38,000	38,000

Table 7. Computed and measured discharges at the Interstate Highway 10 bridge opening at the West Pearl River

Opening section	Discharge, in cubic feet per second		
	Full-reach model (computed)	Local model (computed)[1]	Measured
Left overbank	10,000	10,700	11,300
Channel	16,900	15,600	19,700
Right overbank	11,000	10,100	9,800
Total[2]	37,900	36,400	40,800

[1]Computed using the average discharge across two continuity-check lines

[2]The reason for the discrepancy among the total computed discharges and the total inflow is discussed in the section, "Numerical Solution of the Flow Equations"

After all boundary conditions and roughness types were established, FESWMS was run using the local-model network At the corresponding nodes, the water-surface elevations obtained using the local model are within ±0.2 ft of those obtained using the full-reach model

The discharge distribution at the West Pearl River opening obtained from the local-model calibration simulation closely matches the discharge distribution obtained from the full-reach calibration simulation (table 7) The total discharges obtained from the calibration simulations using the full-reach and local models are 7 and 11 percent, respectively, less than the measured discharge at the West Pearl River opening The reason for the discrepancy between the total computed discharges through the West Pearl River opening and the inflow listed in table 6 is discussed in the section "Numerical Solution of the Flow Equations"

Thus, a comparison of local-model and full-reach model results indicates that two slightly different but equivalent networks of the same area provide similar computed discharge distributions and water-surface elevations. In the following sections, the seven alternatives simulated using the local network are discussed. Water-surface elevations are given to the nearest 0 01 ft for the purpose of comparing differences among alternatives, but accuracy to 0 01 ft is not implied

Simulations of Alternatives 1–3, Requiring Removal of Vegetation

After the local model was adjusted to give results matching closely the results from the full-reach simulation, seven alternatives were simulated. In the first three alternative simulations, brush and trees were cleared on 31, 76, and 167 acres, respectively, in and near the West Pearl River bridge right-of-way as shown in figure 12. To simulate clearing, the Chézy coefficients corresponding to the elements in the cleared areas were assigned the value of 40 $ft^{1/2}/s$, which is recommended by Chow (1959)

The alternatives involving clearing allow more water to flow across the overbanks, while the discharge in the main channel is reduced (table 8). The discharge on the left overbank increases, as a percentage of the computed discharge from the local-model calibration simulation, by 21, 14, and 12 percent for the small, midsize, and large cleared areas, respectively. The discharge on the right overbank increases, as a percentage of the computed discharge from the local-model calibration simulation, by 4 percent for the small cleared area and 11 percent for the midsize and large cleared areas.

The average velocity on the left overbank increases by 0.5 ft/s for all three clearing patterns (table 9). The average velocity on the right overbank increases by 0.1 ft/s for the small cleared area and 0.2 ft/s for the midsize and large cleared areas. Conversely, a decrease in average velocity occurs in the main channel for all three clearing alternatives. The increase in average velocities on the overbanks is caused by a reduction in the resistance to the flow and a reduction in the cross-sectional area needed to convey the discharge on the overbanks

The computed water-surface elevations and backwater for two locations along the western boundary of the local model (fig 12) are listed in table 10. These two locations are significant because the River Gardens subdivision sustained heavy flood damage in April 1980 and Crawford Landing is located in the area of maximum backwater at the west edge of the flood plain

The reduction in backwater at a given location can be compared with the acreage cleared to obtain a reduction in backwater per acres of cleared land. The small, midsize, and large clearing alternatives reduce backwater at Crawford Landing by 0 22, 0.57, and 0.71 ft, respectively, or by 0 07, 0 08, and 0.04 ft, respectively, for every 10 acres cleared. Thus, keeping in mind that the inflow discharge

Table 8. Computed local-model discharges at the Interstate Highway 10 bridge opening at the West Pearl River for existing conditions and seven alternative modifications of the highway crossing

Condition	Discharge,[1] in cubic feet per second			
	Left overbank	Main channel	Right overbank	Total[2]
Existing conditions (calibration)---------	10,700	15,600	10,100	36,400
Simulated condition				
1 Small area (31 acres) cleared at West Pearl River----------	12,900	14,200	10,500	37,600
2 Midsize area (76 acres) cleared at West Pearl River----------	12,200	14,000	11,200	37,400
3 Large area (167 acres) cleared at West Pearl River----------	12,000	14,200	11,200	37,400
4 Right-of-way cleared and ground-surface elevation lowered to elevation of surrounding flood plain----------	13,800	12,800	10,800	37,400
5 Same as 4 with ground-surface elevation lowered to sea level in right-of-way----------	15,200	11,600	11,400	38,200
6 Same as 4 with knoll removed and ground-surface elevation between knoll and river lowered to elevation of surrounding flood plain----------	18,200	11,200	8,400	37,800
7 Same as 4 with discharge reduced to simulate installation of culverts----------	11,800	11,200	9,390	32,400

[1]Computed using the average discharge across two continuity-check lines

[2]The reason for the discrepancy among the total computed discharges and the total inflow is discussed in the section, "Numerical Solution of the Flow Equations"

is fixed in the local-model simulations, if reduction in backwater is the main objective, these three clearing simulations indicate that there is an optimal clearing size. Beyond the optimal clearing size, any additional cleared acreage produces only a marginal reduction in backwater.

Simulations of Alternatives 4–6, Requiring Removal of Spoil

Three alternatives requiring spoil removal were simulated using the local model. The decision to run these three alternatives was based on the hypothesis that spoil removal would significantly reduce backwater for a flood of the magnitude of the April 1980 flood.

To simulate alternative 4 using the local model, model ground-surface elevations on the left overbank, which ranged from 9.0 to 4.0 ft above sea level, were lowered to 2.5 ft above sea level, which is the elevation of the surrounding flood plain. Ground-surface elevations on the right overbank were lowered from 4.0 ft above sea level to 2.5 ft above sea level. The area within the bridge right-of-way was cleared of vegetation. The Chézy coefficients of elements in the cleared area were assigned the value of 40 $ft^{1/2}/s$. The values of all other roughness types remained the same as those used in the local-model calibration simulation

Alternative 4 results in an increase in discharge on both overbanks and a decrease in discharge in the main channel (table 8). Discharge increases 29 percent on the left overbank and 7 percent on the right overbank, as a percentage of the corresponding computed discharge from the local-model calibration simulation. The computed discharge in the main channel is 18 percent less than the computed discharge for the main channel in the local-model calibration simulation. Much of the increase in discharge on the left overbank was obtained by removing the relatively large spoil pile that impedes the flow across this overbank and thus greatly increases the cross-sectional flow area. Compared with the local-model calibration

Table 9. Computed local-model average velocities through the Interstate Highway 10 bridge opening at the West Pearl River for existing conditions and seven alternative modifications of the highway crossing

Condition	Average velocity, in feet per second		
	Left overbank	Main channel	Right overbank
Existing conditions (calibration)	2.0	3.4	1.3
Simulated condition			
1 Small area cleared at West Pearl River	2.5	3.2	1.4
2 Midsize area cleared at West Pearl River	2.5	3.1	1.5
3 Large area cleared at West Pearl River	2.5	3.2	1.5
4 Right-of-way cleared and ground-surface elevation lowered to elevation of surrounding flood plain	1.6	2.8	1.2
5. Same as 4 with ground-surface elevation lowered to sea level in right-of-way	1.4	2.5	1.0
6 Same as 4 with knoll removed and ground-surface elevation between knoll and river lowered to elevation of surrounding flood plain	2.2	2.5	0.9
7 Same as 4 with discharge reduced to simulate installation of culverts	1.4	2.5	1.0

Table 10. Computed local-model water-surface elevations and backwater with the Interstate Highway 10 embankment in place for existing conditions and seven alternative modifications of the highway crossing

Condition	Water-surface elevation,[1] in feet above sea level (Backwater,[2] in feet)	
	Crawford Landing	River Gardens subdivision
Existing conditions (calibration)	12.72 (1.46)	12.92 (1.42)
Simulated condition		
1 Small area cleared at West Pearl River	12.50 (1.24)	12.71 (1.21)
2 Midsize area cleared at West Pearl River	12.15 (0.89)	12.38 (0.88)
3 Large area cleared at West Pearl River.	12.01 (0.75)	12.23 (0.73)
4 Right-of-way cleared and ground-surface elevations lowered to elevation of surrounding flood plain	12.45 (1.19)	12.66 (1.16)
5. Same as 4 with ground-surface elevations lowered to sea level in right-of-way.	12.39 (1.13)	12.60 (1.10)
6. Same as 4 with knoll removed and ground-surface elevations between knoll and river lowered to elevation of surrounding flood plain	11.99 (0.73)	12.23 (0.73)
7. Same as 4 with discharge reduced to simulate installation of culverts	12.03 (0.77)	12.21 (0.71)

[1]Water-surface elevations were obtained from local-model simulations.

[2]Because the local model cannot be meaningfully run without the highway embankments, backwater is computed by assuming that the backwater for the simulation with existing conditions is 1.46 feet at Crawford Landing and 1.42 feet at River Gardens subdivision These values were obtained from full-reach simulations

simulation, the cross-sectional flow area on the left overbank in the alternative 4 simulation is 58 percent larger, whereas the flow area on the right overbank is 19 percent larger.

The average velocities, listed in table 9, decrease on both overbanks and in the main channel Thus, alternative 4 allows the same discharge to be conveyed at a lower average velocity. The decrease in average velocity is greater on the left overbank (0.4 ft/s) than on the right overbank (0.1 ft/s) because of the relatively larger increase in cross-sectional flow area on the left overbank.

Computed water-surface elevations and backwater are given in table 10. At Crawford Landing, backwater is 0.27 ft less in the alternative 4 simulation than in the calibration simulation.

Lowering the ground-surface elevation of nodes in the bridge right-of-way to sea level was simulated in alternative 5. Elements in the bridge right-of-way were assigned a Chézy value of 40 $ft^{1/2}/s$.

The discharge distribution for the alternative 5 simulation is similar to that obtained in the alternative 4 simulation (table 8) Discharge increases 42 and 13 percent on the left and right overbanks, respectively, as a percentage of the corresponding computed discharge in the local-model calibration simulation The discharge in the main channel decreases 26 percent compared with the computed main-channel discharge in the local-model calibration simulation

Computed water-surface elevations and backwater are given in table 10 At Crawford Landing, backwater is 0.33 ft less in the alternative 5 simulation than in the calibration simulation.

Even though the discharge on the overbanks is greater in alternative 5 than in alternative 4, the average velocities on the overbanks (table 9) are lower in alternative 5. Thus, the increase in cross-sectional flow area more than compensates for the increase in discharge on the overbanks to produce the lower average velocities in alternative 5.

The incremental change in the discharge distribution, which results from lowering ground-surface elevations in the bridge right-of-way from 2 5 ft above sea level to sea level, can be obtained by comparing alternatives 4 and 5. The discharges on the left and right overbanks in the alternative 5 simulation increase 10 and 6 percent, respectively, as percentages of the corresponding computed discharges in alternative 4

The incremental effect of lowering the ground-surface elevations in the bridge right-of-way from the elevation of the surrounding flood plain (alternative 4) to sea level (alternative 5) is obtained by subtracting the water-surface elevations computed in alternative 4 from those computed at corresponding nodes in alternative 5. The lowering of ground-surface elevation to sea level produces an incremental lowering of 0.06 ft in the computed water-surface elevation at both Crawford Landing and River Gardens subdivision. This 0.06-f t reduction in backwater is achieved by increasing the cross-sectional flow areas on the left and right overbanks in alternative 5 by 29 and 27 percent, respectively, as percentages of the corresponding cross-sectional areas in alternative 4

The removal of both spoil in the West Pearl River bridge right-of-way and a knoll that protrudes into the flow-expansion zone downstream from the bridge was simulated in alternative 6 Spoil material between the river and the knoll, apparently left after construction, was also removed in this simulation. All ground-surface elevations at nodes in the areas where spoil was removed were lowered to the elevation of the surrounding flood plain

Removal of the knoll increased the cross-sectional area on the left overbank, resulting in a redistribution of flow through the bridge opening Flow on the left overbank increases 70 percent, as a percentage of the corresponding computed discharge in the local-model calibration simulation (table 8), but decreases 28 percent in the main channel and 17 percent on the right overbank. Even though spoil was removed in the bridge right-of-way, the increase in discharge on the left overbank more than compensates for the increase in cross-sectional flow area there, resulting in a higher average velocity (table 9) Thus, these results indicate that the knoll causes a major constriction of flow on the left overbank.

Computed water-surface elevations and backwater are given in table 10 At Crawford Landing, backwater is 0.73 ft less in the alternative 6 simulation than in the calibration simulation.

Simulation of Alternative 7, Requiring Installation of Culverts

Alternative 7 was the same as alternative 4 except for a reduction in inflow to simulate the installation of culverts in the I-10 embankment between the West Pearl and Middle Rivers. Alternative 7 was based on the following assumptions: (1) 40 concrete culverts, each 5 ft in diameter, were installed; (2) each culvert was designed and maintained to minimize energy losses; (3) observed headwater and tailwater elevations for the flood of April 1980 were used, and (4) the entire discharge reduction achieved by installing the culverts occurred at the West Pearl River opening. On the basis of these assumptions and field data from the April 1980 flood, a discharge of 122 ft^3/s was computed for each culvert, giving a total discharge of 4,900 ft^3/s for 40 culverts

The upstream inflow was uniformly lowered to account for the 4,900 ft^3/s reduction in discharge. Ground-surface elevations in the bridge right-of-way and the values of Chézy coefficients were the same as in alternative 4. Water-surface elevations at the downstream boundary, required as model input, were the same as those computed in the full-reach calibration simulation

In the simulation of alternative 7, the discharge decreases 4,400 ft^3/s in the main channel and 710 ft^3/s on the right overbank but, interestingly, increases 1,100 ft^3/s on the left overbank (table 8). Even though the total discharge through the West Pearl River bridge opening is reduced 4,900 ft^3/s, the removal of spoil on the left overbank more than compensates for the reduction in total discharge to produce the increase in discharge on the left overbank

Compared with the calibration simulation, this alternative results in lower average velocities on both overbanks and in the main channel (table 9). Average velocities in alternative 7 are the same as in alternative 5 and the same as or lower than those in all other alternative simulations except the computed average velocity on the right overbank in alternative 6.

Computed water-surface elevations and backwater are given in table 10 At Crawford Landing, backwater is

0 69 ft less in the alternative 7 simulation than in the calibration simulation

Comparison Among Alternatives

Two greatly different flood-plain modifications can produce similar reductions in both backwater and average velocities. For example, alternative 3 involved clearing of vegetation and alternative 6 involved removal of a knoll and the spoil adjacent to the knoll Simulation of these two alternatives produced almost identical computed water-surface elevations and backwater (table 10). Although not identical, the average velocities are similar (table 9). Another example of obtaining similar computed water-surface elevations and backwater by implementing different alternative modifications is shown by comparison of alternatives 6 and 7

Comparison of different alternative simulations also reveals that the same reduction in backwater was obtained with different average velocities; conversely, the same average velocities were obtained with different reductions in backwater. For example, alternatives 4 and 1 have similar computed water-surface elevations but different average velocities (tables 9, 10). Alternatives 5 and 7 have different computed water-surface elevations and identical average velocities.

Thus, the local-model results show that the selection of an alternative modification should be based on the intended objective, whether it be a reduction in backwater, a reduction in average velocity, or a combination of the two. On the basis of the results of the local model and the objective of lowering backwater without increasing average velocities, four alternatives were selected for study using the larger network discussed in the following section.

SIMULATION OF FOUR MODIFICATIONS OF INTERSTATE HIGHWAY 10 FOR THE APRIL 2, 1980, FLOOD

The four alternative modifications of the I-10 crossing include: (1) improving the hydraulic characteristics of the three bridge openings by removing spoil, natural levees, and vegetation; (2) placing a new 2,000-ft bridge opening in the crossing and clearing brush and trees from an area 1,000 ft wide and 3,000 ft long, centered along the new bridge with the long side parallel to the roadway; (3) placing a new 2,000-ft bridge opening in the crossing and clearing brush and trees only in the new bridge right-of-way, and (4) placing a 1,000-ft bridge opening in the crossing and clearing brush and trees only in the new bridge right-of-way. The networks used to simulate all four alternatives were identical to the middle part of the full-reach network (fig. 4) except for slight modifications required to represent each alternative Network modifications, results of the simulation, backwater, and drawdown are discussed for each alternative modification Model results are used to evaluate each alternative with respect to three objectives: (1) reducing backwater caused by the I-10 crossing, (2) eliminating overtopping of the roadway, and (3) decreasing velocities in the bridge openings.

Results obtained from an alternative simulation using this network will differ slightly from results obtained from the same alternative simulation using the full-reach network This difference in computed results is caused by the close proximity of the upstream and downstream boundaries to the highway crossing. Boundary conditions, obtained from the results of the full-reach calibration simulation and held fixed in the alternative simulations, would actually be slightly different owing to the alternative modifications at and near I-10.

Boundary Conditions

Boundary conditions for the four alternative simulations were obtained from the calibration simulation of the full-reach model developed by Lee and others (1983). At the upstream boundary, the unit discharges required as input for the four alternative simulations were taken from corresponding nodes from the calibration simulation of the full study reach At the upstream boundary, input discharge at the Pearl and West Pearl Rivers was 8,090 and 6,040 ft^3/s, respectively. The remaining 154,000 ft^3/s was distributed uniformly across the flood plain (table 11).

At the downstream boundary, the water-surface elevations were those computed at corresponding nodes in the calibration simulation using the full-reach model. The downstream water-surface elevation ranges from 10.1 ft above sea level at the right edge of the flood plain to 9 6 ft above sea level at the left edge of the flood plain

Table 11. Distribution of discharge at the upstream model boundary for the alternative simulations

Section of upstream boundary	Discharge, in cubic feet per second
Left edge of flood plain to left edge of water of Pearl River	6,720
Pearl River—main channel	8,090
Right edge of water of Pearl River to left edge of water of West Pearl River	143,000
West Pearl River—main channel	6,040
Right edge of water of West Pearl River to right edge of flood plain	3,980
Total	168,000

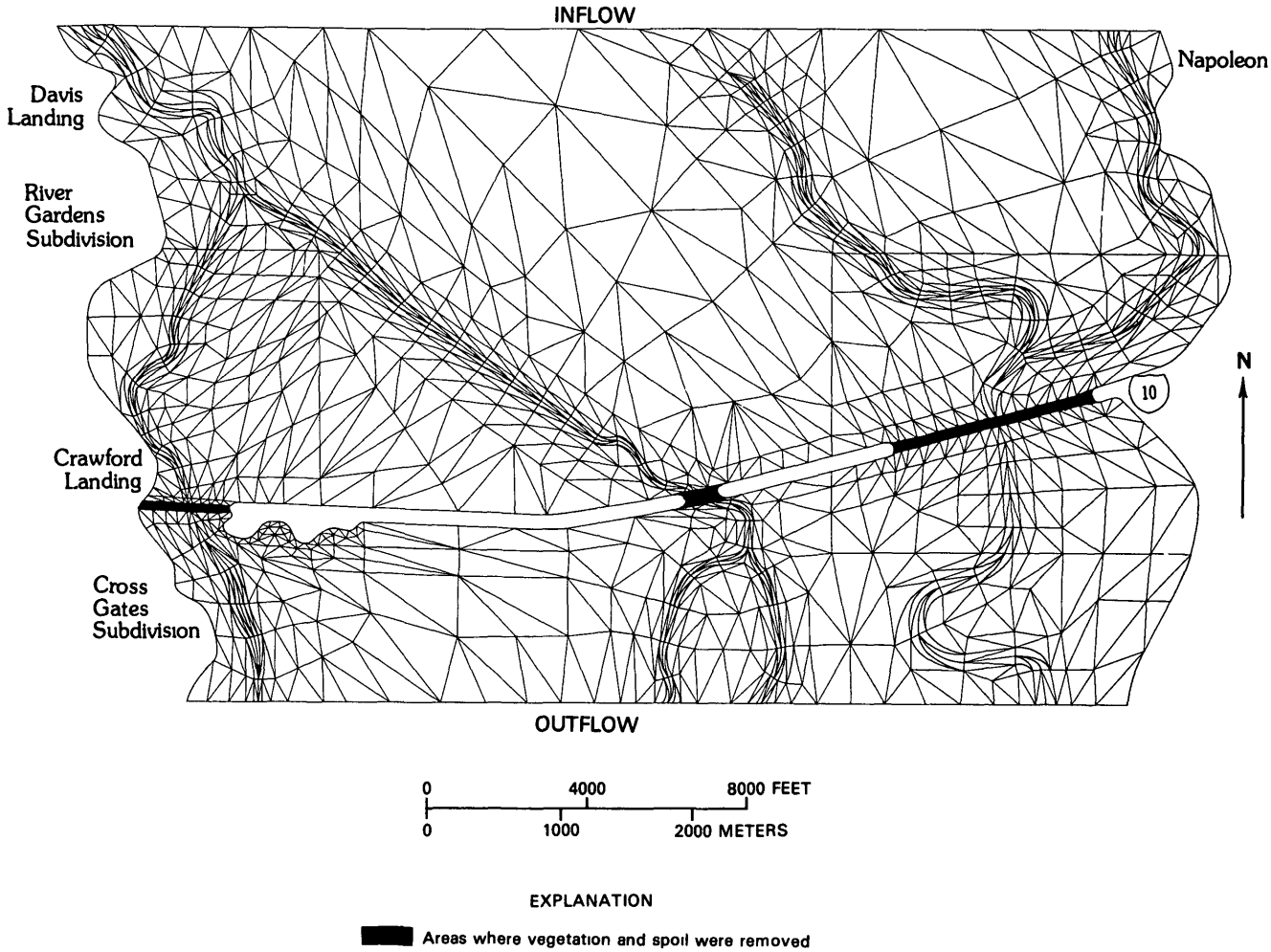

Figure 13. Finite-element network for the alternative 1 simulation

Alternative 1 Simulation

During the model-adjustment process reported by Lee and others (1983) and while conducting the local-model simulations discussed previously, it was observed that computed water-surface elevations were moderately sensitive to the values of the Chézy coefficients of the overbank elements within the three bridge openings. The computed water-surface elevations were also sensitive to model ground-surface elevations within and near the bridge rights-of-way. Alternative 1, developed on the basis of these observations, involved modifications to the overbank areas within the bridge rights-of-way. These modifications included removal of spoil left after construction, natural levees along the channels, and brush and trees.

Network and Parameter Modifications

The grid used for alternative 1 was the same as the one shown in figure 4 for the study area. It is shown at a larger scale in figure 13. To simulate alternative 1 using FESWMS, model ground-surface elevations of the overbank areas within the rights-of-way at the three I-10 bridge openings were lowered to the elevation of the surrounding flood plain. Elevations ranging from 2.2 to 4.6 ft above sea level, within the highway right-of-way on the right overbank at the Pearl River, were lowered to 1.5 ft above sea level. No spoil was left after construction on the left overbank of the Pearl River; therefore, no changes were made to ground-surface elevations on this overbank. Ground-surface elevations ranging from 2 5 to 4.0 ft above sea level on both overbanks at the Middle River were lowered to 2.0 ft above sea level Ground-surface elevations on the right overbank of the West Pearl River did not require changing, because no spoil was left after construction, but elevations ranging from 4.0 to 9.0 ft above sea level on the left overbank were lowered to 2.5 ft above sea level. Elevations at and near the knoll southeast of the West Pearl River opening were lowered to the elevation of the surrounding flood plain, 1.5 to 3.0 ft above sea level, and elevations ranging from 5.0 to 8.0 ft above sea level between the knoll and the West Pearl River were lowered to between

Table 12. Values of Chézy coefficients used to simulate the April 2, 1980, flood for existing conditions (calibration) and four alternative modifications of the highway crossing

Element description and location	Chézy coefficient, in foot to the one-half power per second				
		Alternative			
	Calibration	1	2	3	4
Woods	22	22	22	22	22
Marsh grass and brush downstream from Interstate Highway 10 bridge across Pearl River	30	30	30	30	30
Brush and trees south of preceding marsh-grass area	21	21	21	21	21
Grass and scattered brush on left overbank under Interstate Highway 10 bridge across Pearl River	40	40	40	40	40
Grass and brush on right overbank under Interstate Highway 10 bridge across Pearl River	30	40	30	30	30
Brush and trees under Interstate Highway 10 across Middle River	21	40	21	21	21
Grass and scattered brush under Interstate Highway 10 bridge across West Pearl River	40	40	40	40	40
New bridge right-of-way	---	---	40	40	40
Area 1,000-feet-by-3,000-feet adjacent to new bridge right-of-way	22	22	40	22	22
Pearl River, natural channel between river miles 13 5 and 15 9	105	105	105	105	105
Pearl River, natural channel between river miles 15.9 and 18 1	85	85	85	85	85
Wastehouse Bayou, straightened channel between river miles 0 0 and 4 4	59	59	59	59	59
Middle River, straightened channel between river miles 7 3 and 9 0	66	66	66	66	66
Middle River, natural channel between river miles 9 0 and 10 0	85	85	85	85	85
Middle River, straightened channel between river miles 10 0 and 12 9	68	68	68	68	68
West Middle River, straightened channel between river miles 11 3 and 12 7	75	75	75	75	75
West Pearl River, natural channel between river miles 12.3 and 14 9	85	85	85	85	85
West Pearl River, straightened channel between river miles 14 9 and 15 9	51	51	51	51	51
West Pearl River, natural channel between river miles 15 9 and 17 0	100	100	100	100	100

3.0 and 5 0 ft above sea level. Natural-levee ridges along the channel banks, outside of the bridge rights-of-way, were left unchanged.

The Chézy coefficients of the overbank elements in the bridge rights-of-way shown in figure 13 were assigned a value of 40 $ft^{1/2}/s$, which is recommended by Chow (1959) for a vegetative cover of short grass with no brush (table 12). As indicated by the values of the Chézy coefficients listed in table 12, the Middle River has the most dense vegetative cover (brush and trees) of the three bridge openings The scattered brush under the I-10 bridge across the West Pearl River and on the left overbank of the Pearl River did not require a change in the value of the Chézy coefficient.

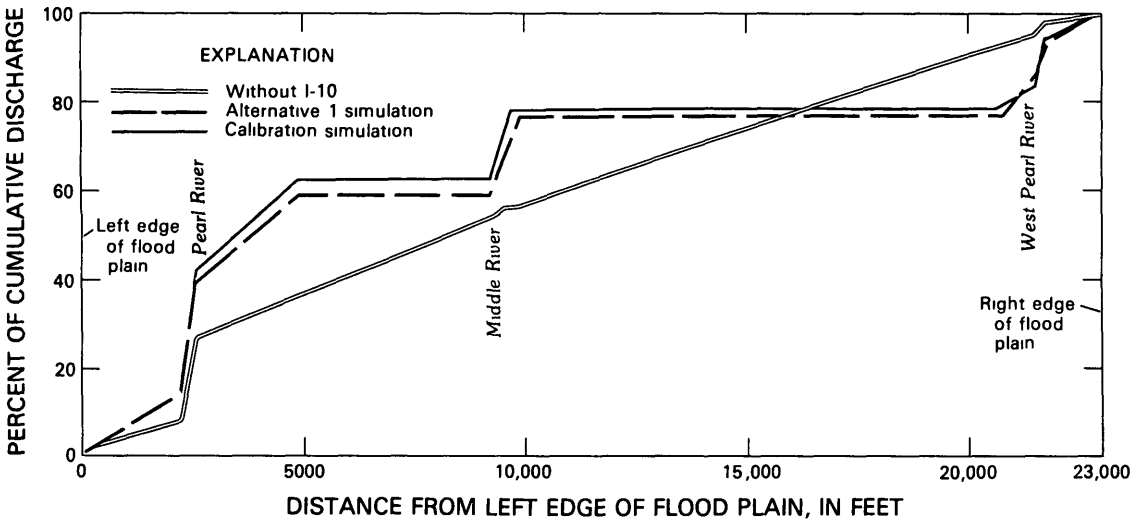

Figure 14. Distribution of discharge across the flood plain at Interstate Highway 10 for alternative 1

Results of the Simulation

Alternative 1 was simulated using the network shown in figure 13. In general, compared with the calibration simulation, the velocity field for alternative 1 has a more southerly flow component (pl. 1). Near I-10 the flow converges toward the three openings, flows through the openings, and then diverges out of the main channels back onto the flood plain. At the downstream boundary, the flow is almost uniformly distributed across the flood plain and the velocity field has a south-southeasterly component similar to that of the calibration simulation.

Table 13. Computed water-surface elevations and backwater or drawdown for existing conditions and four alternative modifications of the highway crossing

Reference number and location on plates	Water-surface elevation, in feet above sea level (backwater) or [drawdown], in feet					
	With highway embankments	Without highway embankments	Alternative 1	Alternative 2	Alternative 3	Alternative 4
1 Davis Landing----------	13 8 (0 9)	12 9	13 5 (0 6)	13 0 (0 1)	13 0 (0 1)	13 1 (0 2)
2 Napoleon----------	12 8 (1 1)	11 7	12 4 (0 7)	12 0 (0.3)	12 0 (0 3)	12 1 (0 4)
3 River Gardens subdivision----	12 8 (1 4)	11 4	12 4 (1 0)	11 7 (0 3)	11 7 (0 3)	11.9 (0 5)
4 Mouth of Gum Bayou---------	12 7 (1 4)	11 3	12.3 (1 0)	11 6 (0 3)	11 6 (0 3)	11 8 (0.5)
5 West edge of flood plain, 0 2 mile downstream from Interstate Highway 10	10 5 [0 1]	10 6	10 5 [0 1]	10 3 [0 3]	10 3 [0 3]	10 4 [0 3]
6 East edge of flood plain, 0 2 mile downstream from Interstate Highway 10	10 9 (0 6)	10 3	10 8 (0 5)	10 5 (0 2)	10 5 (0 2)	10 6 (0 3)
7. East edge of flood plain, 0.7 mile downstream from Interstate Highway 10	10.8 (0 6)	10 2	10 7 (0 5)	10 4 (0 2)	10 4 (0 2)	10 5 (0 3)

The distribution of discharge across the flood plain is shown in figure 14. This figure shows that without I-10 there is a relatively uniform increase in cumulative discharge across the flood plain. The only sharp break in the slope of the line, which corresponds to a rapid increase in cumulative discharge, occurs at the Pearl River Without I-10 in place, the main channels of the Middle and West Pearl Rivers convey a small percentage of the total discharge. The line representing the cumulative discharge with I-10 in place graphically depicts the large percentage of water that is transferred across the flood plain and flows through the Pearl River opening As this transfer of water from the west to the east side of the flood plain is reduced, the plotted line for a given alternative simulation will better approach the plotted line representing the distribution without I-10. Thus, alternative 1 reduces the transfer of water across the flood plain, and the plotted line is closer to that for the simulation without I-10

The computed water-surface elevations are shown by contours on plate 1 and are tabulated in table 13 Upstream from the I-10 embankment, the alternative 1 simulation reduces the computed water-surface elevations by approximately 0.4 ft compared with the calibrated water-surface elevations. At the western upstream boundary of the study area, near Davis Landing, the water-surface elevation is 1 3 ft higher on the west side of the flood plain than on the east side. Along the east edge of the flood plain, approximately 0.2 mi downstream from the Pearl River bridge (location 6), the computed water-surface elevation is 0.1 ft less than the computed water-surface elevation with I-10 in place. At the west edge of the flood plain, 0.2 mi downstream from the West Pearl River bridge, the computed water-surface is the same as the computed water-surface elevation with I-10 in place.

The computed discharges at each of the three bridge openings are given in table 14. The discharges were obtained from continuity checks along the line of nodes closest to the south edge of the eastbound lane, where the measured discharges were obtained. The discharge in the main channel (as a percentage of the computed discharge in the

Table 14. Computed discharges at the Interstate Highway 10 bridge openings for existing conditions and four alternative modifications of the highway crossing

Opening section	Discharge, in cubic feet per second				
	Existing conditions (calibration)	Alternative			
		1	2	3	4
Pearl River					
Left overbank	23,600	24,900	17,400	17,800	18,500
Channel	50,200	40,600	39,100	40,300	41,700
Right overbank	36,100	36,200	26,400	27,300	28,600
Subtotal	110,000	102,000	82,900	85,400	88,800
Middle River					
Left overbank	3,810	6,050	2,380	2,490	2,650
Channel	17,800	16,300	11,500	11,800	12,800
Right overbank	5,360	9,000	3,340	3,470	3,760
Subtotal	27,000	31,400	17,200	17,800	19,200
West Pearl River					
Left overbank	10,000	11,800	5,660	6,020	6,680
Channel	16,900	14,100	10,600	11,300	12,300
Right overbank	11,000	11,000	6,620	6,920	7,530
Subtotal	37,900	36,900	22,900	24,200	26,500
New bridge opening					
Flood plain	-------	---------	41,000	38,700	36,600
Total[1]	175,000	170,000	164,000	166,000	171,000

[1]The reason for the discrepancy among the total computed discharges and the total inflow is discussed in the section, "Numerical Solution of the Flow Equations "

Table 15. Computed average velocities at the Interstate Highway 10 bridge openings for existing conditions and four alternative modifications of the highway crossing

Opening section	Velocities, in feet per second				
	Existing conditions (calibration)	Alternative			
		1	2	3	4
Pearl River					
Left overbank	15	12	12	12	13
Channel	36	29	2.8	29	30
Right overbank	18	1.5	15	15	16
Overall average	23	18	18	1.8	19
Middle River					
Left overbank	2.6	29	17	18	19
Channel	43	36	29	30	32
Right overbank	32	38	22	23	24
Overall average	37	35	25	26	27
West Pearl River					
Left overbank	23	16	15	16	17
Channel	35	28	23	24	26
Right overbank	14	10	09	09	10
Overall average	22	16	15	1.5	17
New bridge opening					
Flood plain	-------	---------	20	19	34

calibration simulation) decreases 19, 8, and 17 percent at the Pearl, Middle, and West Pearl Rivers, respectively. Discharge increases on all overbanks, except on the right overbank of the West Pearl River, where it remains unchanged. The increase in discharge on the left overbank at the West Pearl River opening is caused by lower ground-surface elevations within the bridge right-of-way; at the Middle and Pearl Rivers, the increase is caused by lower ground-surface elevations and a reduction in resistance. Total discharge through an opening decreases at the Pearl and West Pearl River openings, and most of the 4,400 ft^3/s increase in discharge at the Middle River is captured from the Pearl River opening

The average velocities for the main channel and overbanks for the three bridge openings computed in the calibration and alternative 1 simulations are listed in table 15 and are plotted on figures 15*A*, 16*A*, and 17*A*. Average velocities decrease on the overbanks and in the main channel at the Pearl River opening The unit discharges (fig 15*B*) also decrease on the overbanks and in the main channel in this opening The decrease in unit discharges in the main channel and across most of both overbanks is caused by a reduction in average velocity. Even though average velocities decrease on the overbanks of the Pearl River, unit discharges increase near the edge of both overbanks. The increase is caused by the removal of spoil, which increases the cross-sectional flow areas and more than compensates for the reduction in resistance.

The average velocity in the main channel of the Middle River decreases from 4.3 to 3.6 ft/s, but the average velocity increases by 0.3 ft/s on the left overbank and by 0.6 ft/s on the right overbank (table 15). The average velocity of 3.8 ft/s on the right overbank of the Middle River is the highest average velocity computed in the alternative 1 simulation. Even though the discharge at the Middle River opening increases, the overall average velocity decreases. The increase in unit discharge on both overbanks of the Middle River, shown in figure 16*B*, is caused by both an increase in cross-sectional flow area due to spoil removal and an increase in average velocity due to a reduction in resistance. The reduction in resistance more than compensates for the increase in cross-sectional flow area, the net result being an increase in average velocity. This reduction in resistance between the calibration simulation and the alternative 1 simulation is greatest on the overbanks at the Middle River (table 12).

At the West Pearl River opening, the average velocities decrease in the main channel and on both overbanks

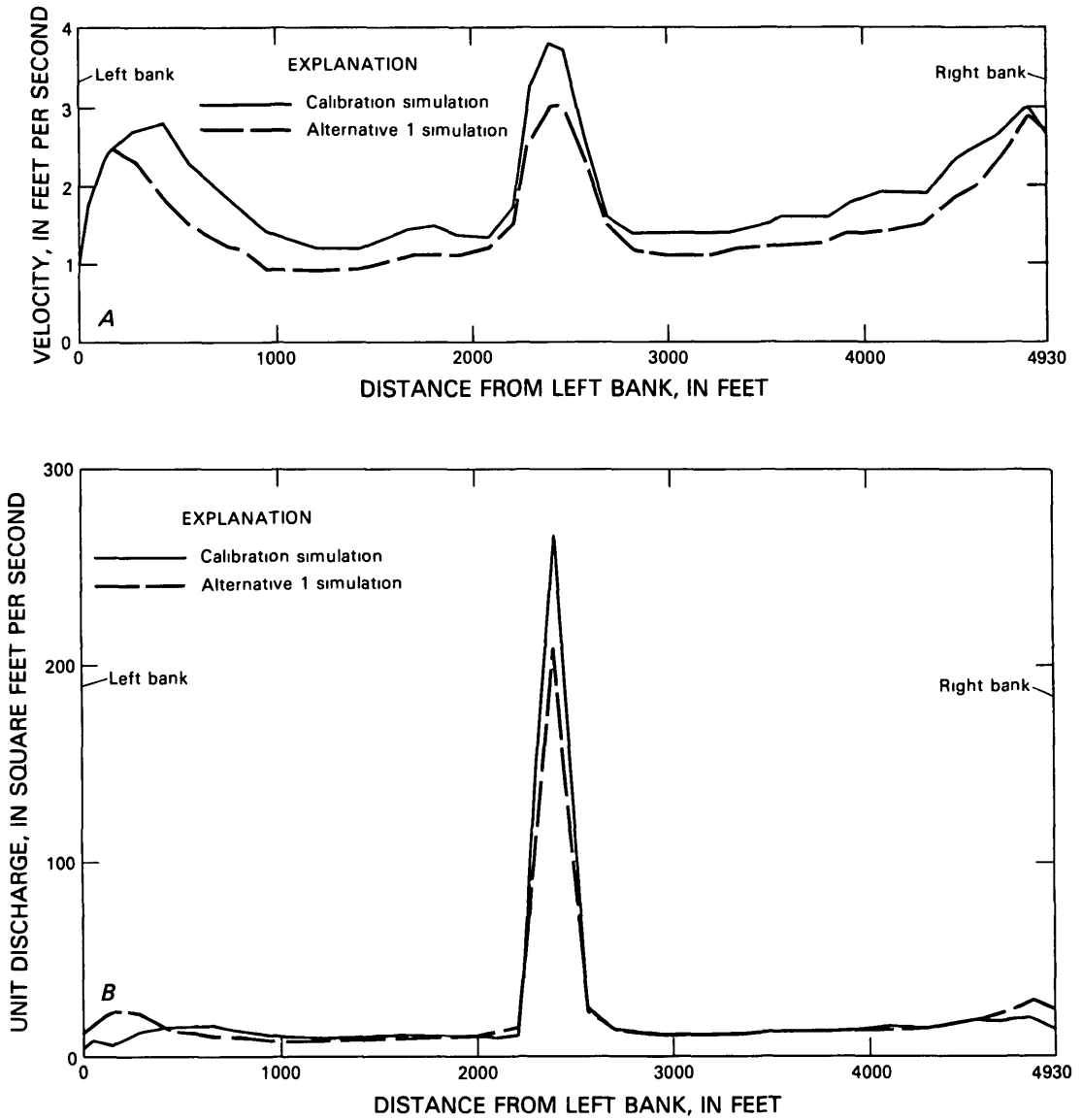

Figure 15. Computed (*A*) average velocities and (*B*) unit discharges for the calibration and alternative 1 simulations at the Interstate Highway 10 bridge opening at the Pearl River

(table 15). The decrease is larger on the left overbank than on the right. The relatively large decrease on the left overbank is caused by a large increase in flow area produced by lowering of ground-surface elevations ranging from 4.0 to 9 0 ft above sea level in the calibration simulation to 2.5 ft above sea level in the alternative 1 simulation. Although the average velocity decreases on the left overbank, the unit discharge increases, as shown in figure 17*B*, owing to the large increase in cross-sectional area.

Lines of equal backwater and drawdown are shown on plate 2. These lines were produced by subtracting nodal water-surface elevations from the simulation without I-10 in place (Lee and others, 1983) from corresponding water-surface elevations computed for alternative 1. Maximum backwater of 1.7 ft occurs on the upstream side of the I-10 embankment between the Middle and West Pearl Rivers. Maximum backwater of 2.1 ft occurred at the same location in the calibration simulation Maximum backwater at the west edge of the flood plain is 1.1 ft near Crawford Landing. Maximum backwater at the east edge of the flood plain is 0.7 ft, 0.3 mi downstream from Napoleon. The corresponding values of backwater in the calibration simulation were 1.5 ft near Crawford Landing and 1.1 ft near Napoleon. Upstream from I-10, backwater decreases more

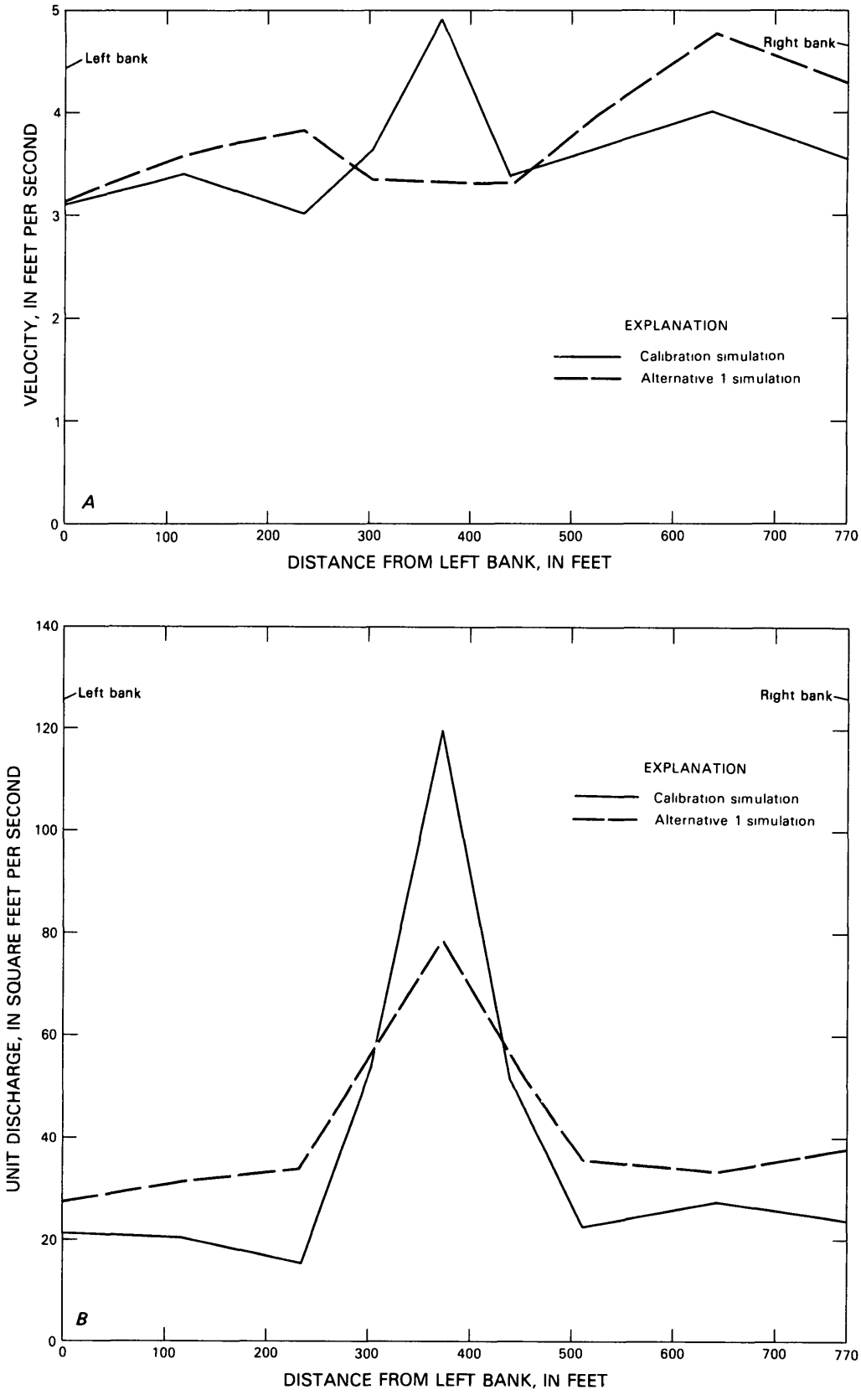

Figure 16. Computed (*A*) average velocities and (*B*) unit discharges for the calibration and alternative 1 simulations at the Interstate Highway 10 bridge opening at the Middle River

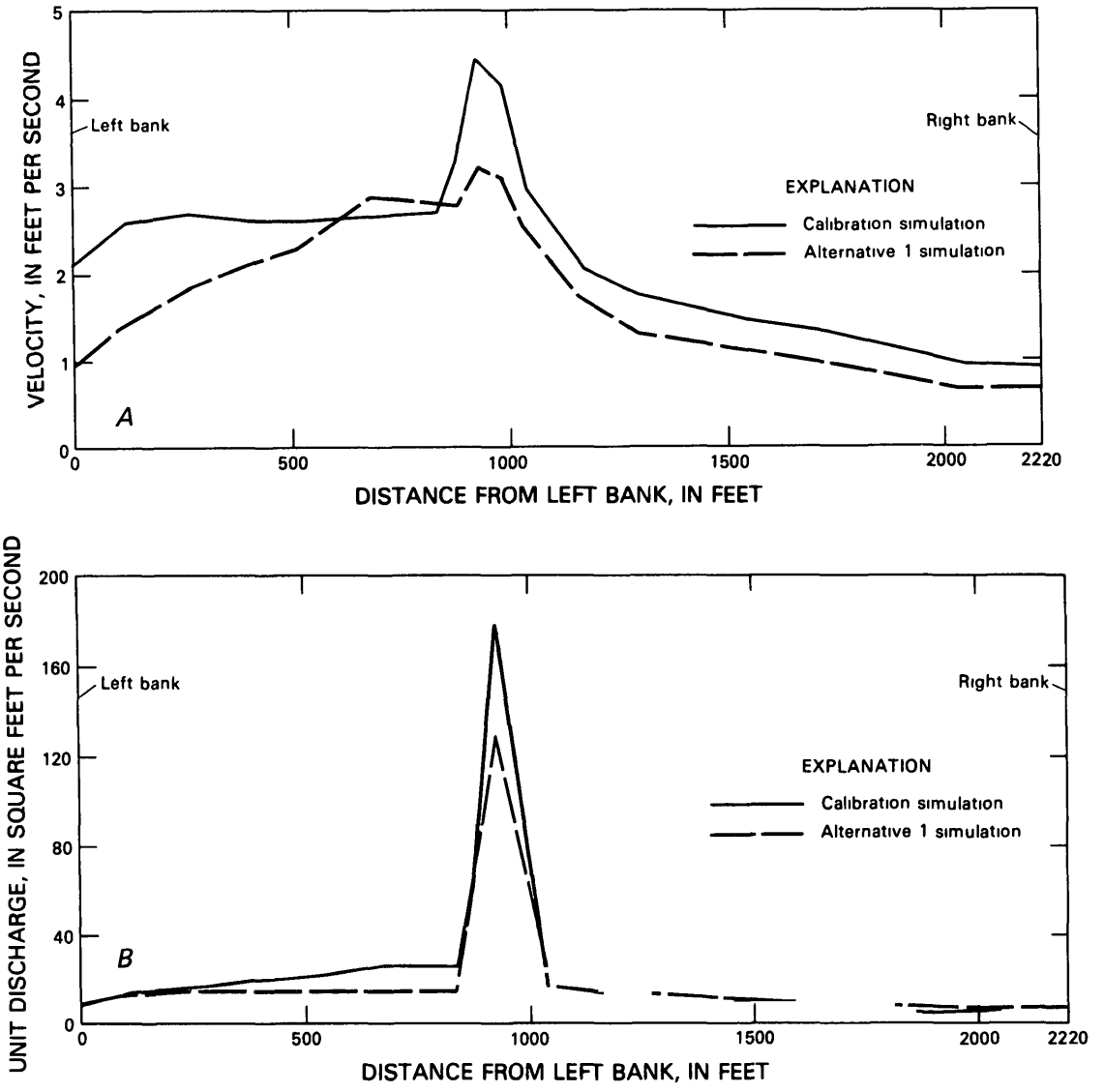

Figure 17. Computed (*A*) average velocities and (*B*) unit discharges for the calibration and alternative 1 simulations at the Interstate Highway 10 bridge opening at the West Pearl River

rapidly in the upstream direction on the west side of the flood plain than on the east side (figs. 18, 19). This is the same pattern as in the calibration simulation.

The water-surface gradients in the Middle and West Pearl River openings are reduced from the calibration values in this simulation but remain larger than the gradient in the Pearl River opening.

Maximum drawdown for alternative 1 of 0.7 ft occurs on the downstream side of the I-10 embankment between the Middle and West Pearl Rivers. Drawdown of 0.2 ft extends 0.5 mi downstream from I-10 at the west edge of the flood plain. On the east side of the flood plain, backwater ranges from 0.5 ft at I-10 to 0.2 ft at the downstream boundary (pl. 2)

On the basis of the results of this simulation, alternative 1 can be evaluated with respect to the three previously mentioned objectives. Alternative 1 reduces backwater by approximately 0.3 to 0.4 ft upstream from I-10. Interstate-10 was overtopped by only a few inches in the April 1980 flood; hence, alternative 1 eliminates the possibility of roadway overtopping for a flood of the magnitude of the 1980 flood. Average velocities in the main channels and on the overbanks at the Pearl and West Pearl River openings are reduced compared with those of the

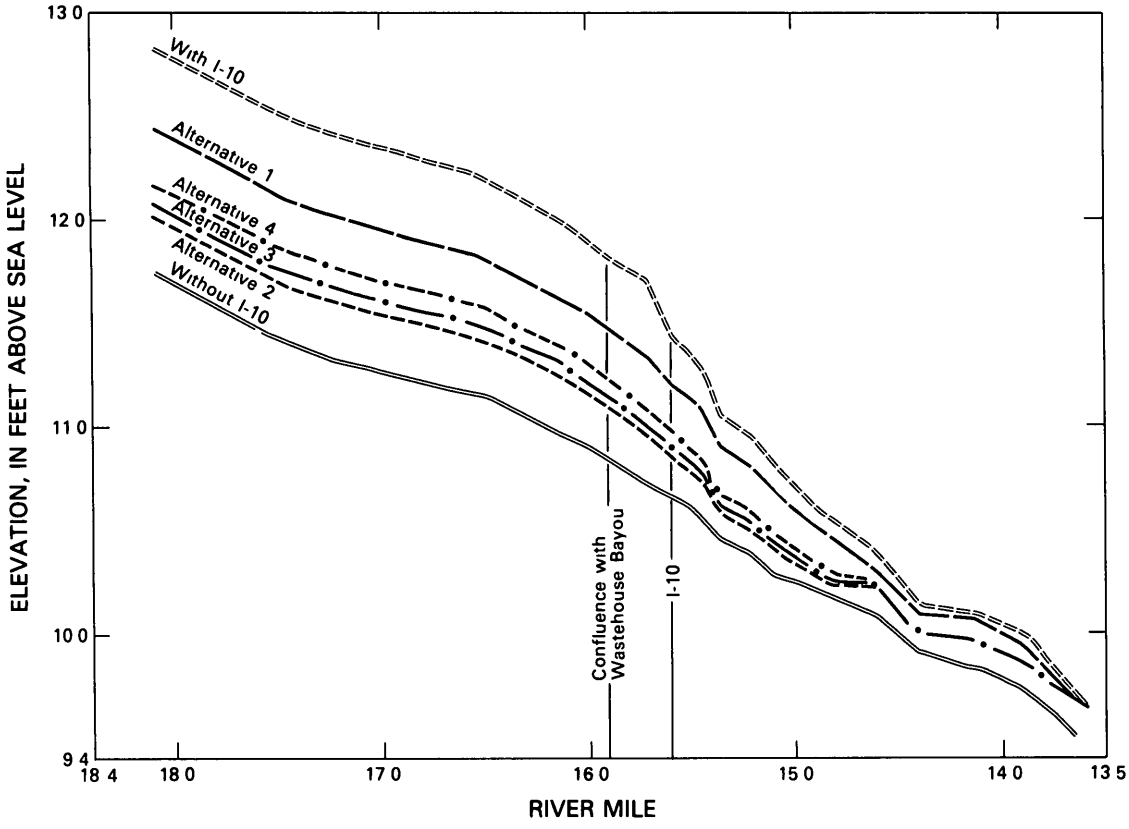

Figure 18. Computed water-surface elevations for the Pearl River, center of channel, for the simulations with Interstate Highway 10, without Interstate Highway 10, and the four alternatives

existing crossing. At the Middle River, average velocities increase on the overbanks and decrease in the main channel. Alternative 1 reduces backwater and lowers the overall bridge-opening velocity at the Middle River, even with an increase in discharge through the opening.

Alternative 2 Simulation

Alternative 2, a new bridge opening, was designed to create the greatest expected reduction in backwater of the four alternatives simulated. To obtain the maximum possible reduction in backwater from a 2,000-ft bridge opening, the new bridge was placed in the I-10 embankment near where maximum backwater was computed in the calibration simulation. Put in another perspective, this alternative was developed to answer the question, how much backwater would have been produced if all existing bridge openings had remained unchanged but an additional 2,000-ft bridge opening had existed in the I-10 embankment? In addition to a new bridge in the embankment, brush and trees were cleared in and near the new bridge opening to further reduce backwater

Network and Parameter Modifications

To simulate alternative 2, the finite-element network was modified, as shown in figure 20, by adding elements to that area of the embankment occupied by the new bridge. Ground-surface elevations at nodes in the new bridge right-of-way were set at sea level. A rectangular area 1,000 ft wide and 3,000 ft long, with the long side parallel to the roadway, was cleared of brush and trees. The Chézy coefficients of elements in the cleared area were assigned the value of 40 $ft^{1/2}/s$ (table 12). At the Pearl, Middle, and West Pearl Rivers, the ground-surface elevations and the values of the Chézy roughness coefficients were identical to those used in the calibration simulation.

Results of the Simulation

The velocity vectors produced in the alternative 2 simulation have a more southerly component throughout the reach modeled, compared with the south-southeasterly component produced in the calibration simulation (pl 3). Alternative 2 significantly reduces the flow shift from the

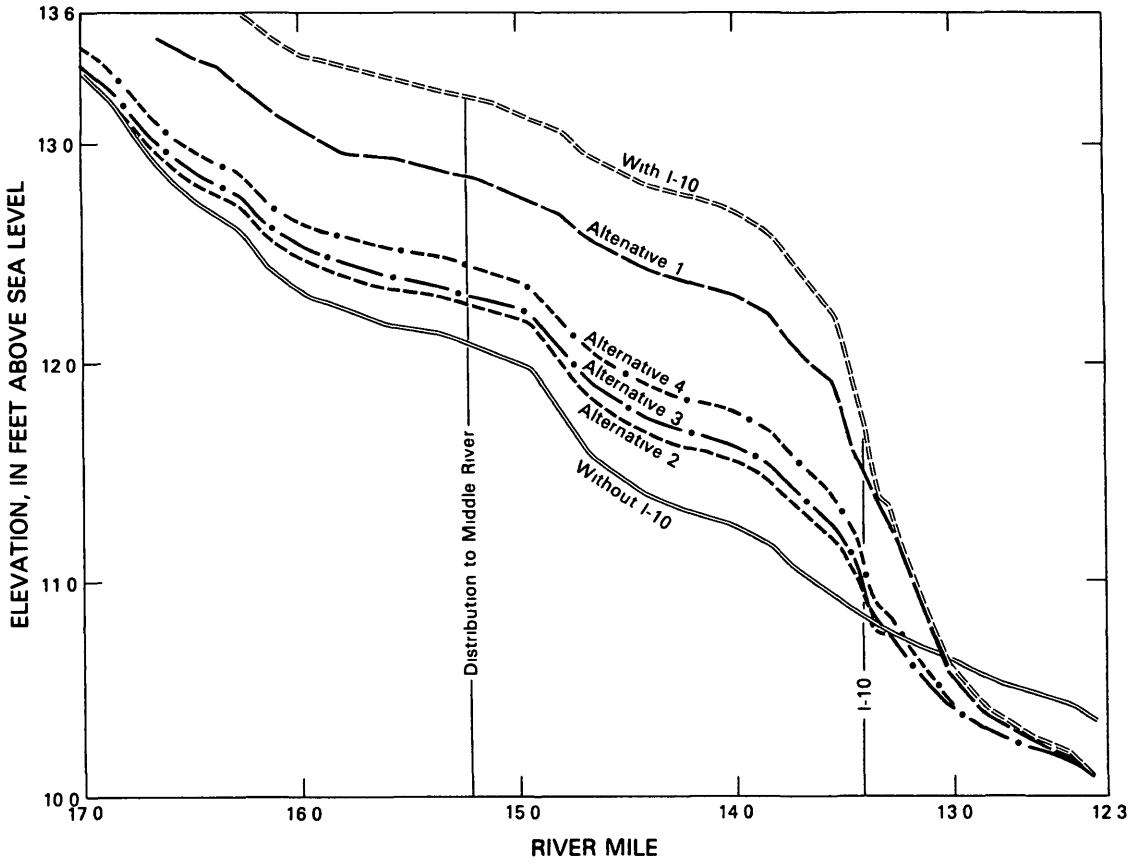

Figure 19. Computed water-surface elevations for the West Pearl River, center of channel, for the simulations with Interstate Highway 10, without Interstate Highway 10, and the four alternatives

west side of the flood plain to the east side upstream from I-10. The cumulative discharge versus distance across the flood plain, plotted in figure 21, shows that the discharge distribution through the four embankment openings more closely corresponds to the discharge distribution without I-10 in place than do the distributions corresponding to any of the other alternatives.

Owing to the added conveyance at the I-10 embankment, convergence toward the I-10 openings and divergence back onto the flood plain occurs in a 0.6-mi-long reach centered about I-10, whereas it occurred in a 3-mi-long reach in the full-study calibration run.

The computed water-surface elevations are shown by contours on plate 3. Upstream from I-10, the computed water-surface elevations are lower than those computed in the calibration simulation. The water-surface elevation at Davis Landing, on the west side of the flood plain, is 1.0 ft higher than the water-surface elevation at Napoleon. The water-surface elevations downstream from I-10, on both sides of the flood plain, are lower than those computed in the calibration simulation (table 13).

The computed discharges at each of the four bridge openings are given in table 14. Alternative 2 reduces the discharge 25, 36, and 40 percent at the Pearl, Middle, and West Pearl Rivers, respectively, as a percentage of the calibrated discharge at each opening. The main channel discharge, as a percentage of the calibrated discharge in each main channel, is reduced 22, 35, and 37 percent at the Pearl, Middle, and West Pearl Rivers, respectively. A decrease in discharge of 26 and 27 percent occurs on the left and right overbanks of the Pearl River opening. Discharge decreases 38 percent on both overbanks of the Middle River. The greatest decreases in discharge, 43 and 40 percent, occur on the left and right overbanks of the West Pearl River, respectively. The new bridge carries 41,000 ft^3/s, or 25 percent of the total computed discharge in the alternative 2 simulation.

The average velocities in the main channel and on the overbanks are reduced at all three openings, as shown in figures 22, 23, and 24, which indicate that a rather uniform reduction in average velocity is achieved across the overbanks at the three openings. The smallest reduction in average velocity (0.3 ft/s) occurs across both

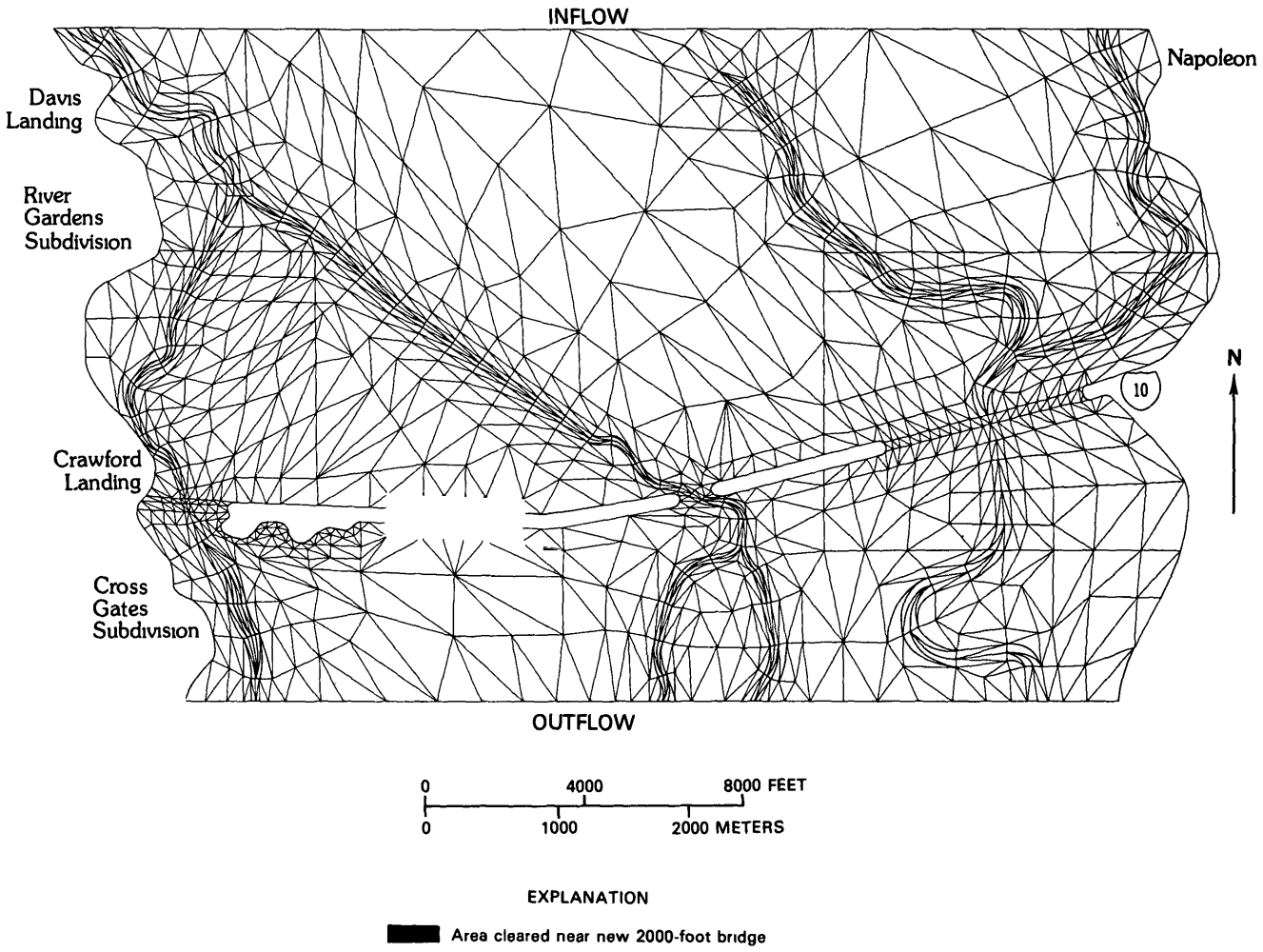

Figure 20. Finite-element network for the alternative 2 and 3 simulations

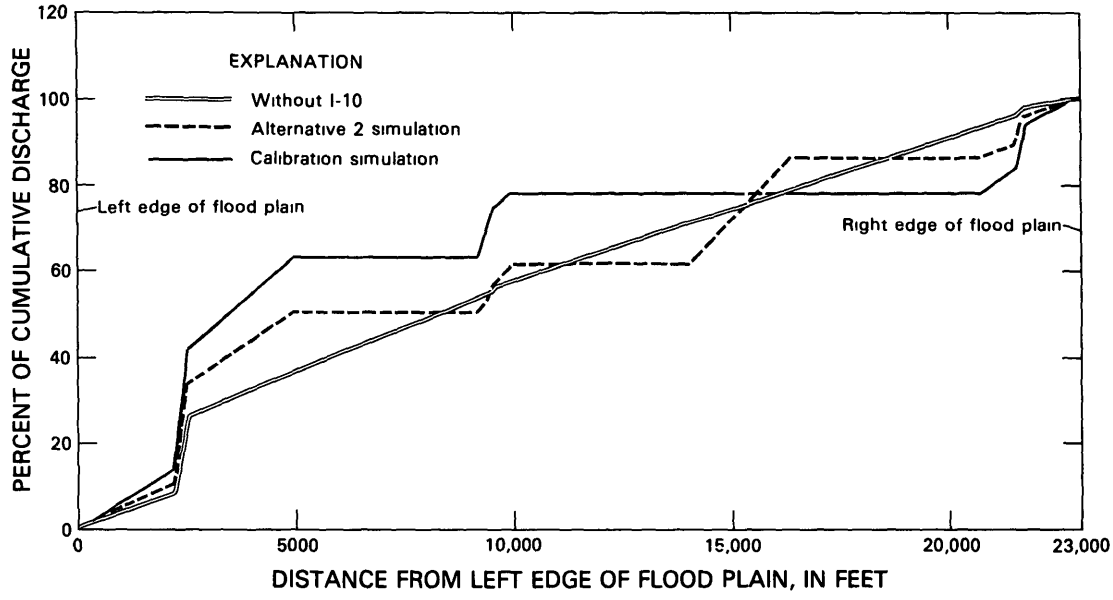

Figure 21. Distribution of discharge across the flood plain at Interstate Highway 10 for alternative 2

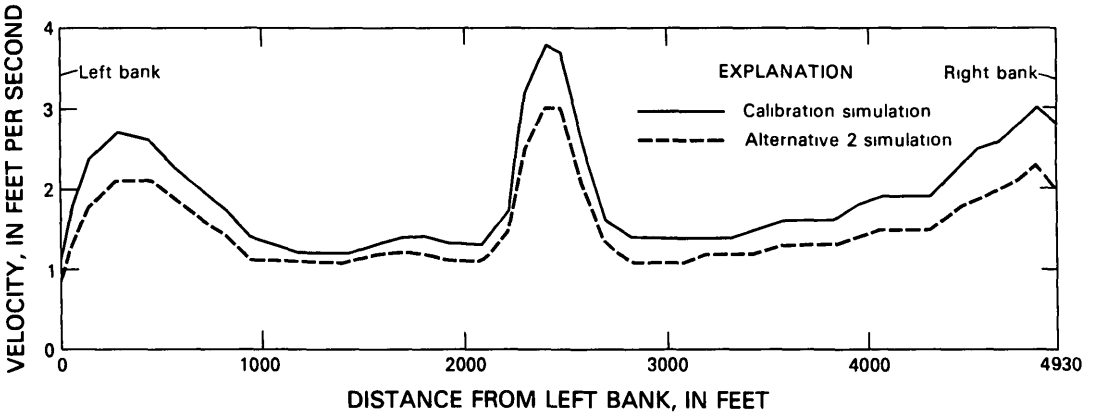

Figure 22. Computed average velocities for the calibration and alternative 2 simulations at the Interstate Highway 10 bridge opening at the Pearl River

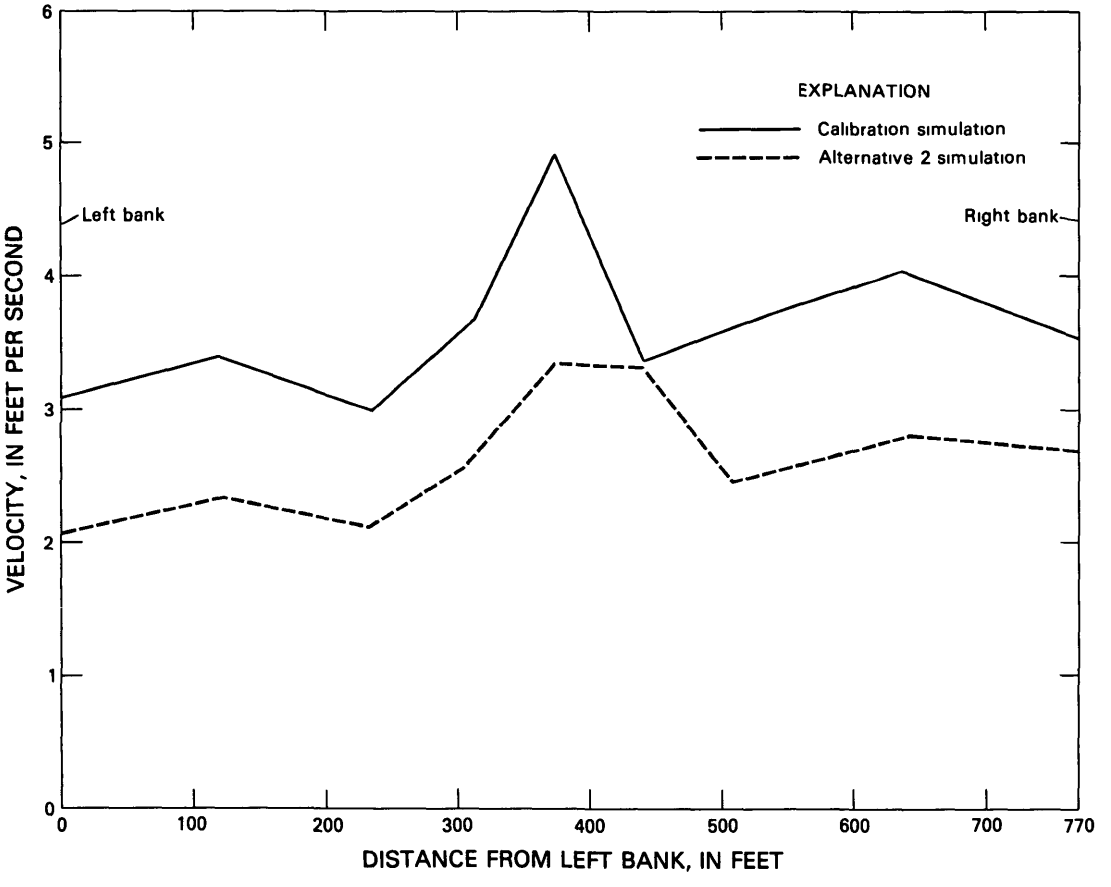

Figure 23. Computed average velocities for the calibration and alternative 2 simulations at the Interstate Highway 10 bridge opening at the Middle River

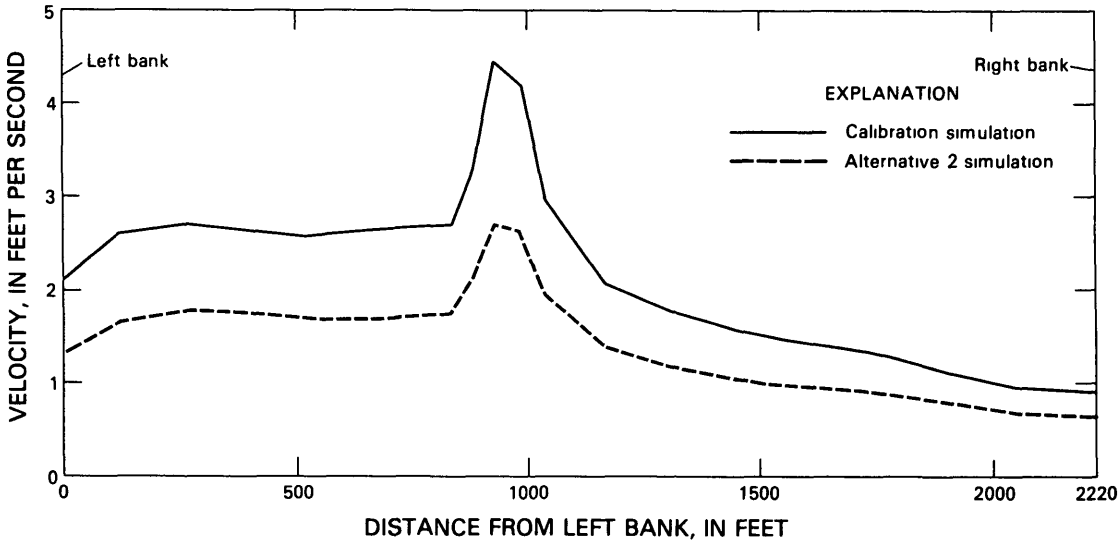

Figure 24. Computed average velocities for the calibration and alternative 2 simulations at the Interstate Highway 10 bridge opening at the West Pearl River

overbanks of the Pearl River (table 15). The largest reduction in average velocity (1.4 ft/s) occurs in the main channel of the Middle River, and the largest overall reduction through an opening (1.2 ft/s) also occurs at the Middle River. Even with the relatively large reduction in average velocity at the Middle River, the highest average velocity (2 5 ft/s) through an opening occurs in the Middle River. At the West Pearl River opening, the decrease in average velocity on the left overbank (0.8 ft/s) is greater than the decrease in average velocity on the right overbank (0.5 ft/s). The average velocity through the new bridge opening is 2.0 ft/s, compared with an average velocity of 0.7 ft/s across the flood plain.

Lines of equal backwater and drawdown for alternative 2 are shown on plate 4. Maximum backwater of 0.7 ft occurs along the upstream side of the I-10 embankment between the Pearl and Middle Rivers, whereas, in the calibration simulation, maximum backwater (2.1 ft) occurred between the Middle and West Pearl Rivers On the east edge of the flood plain, maximum backwater of 0.3 ft occurs from just upstream from I-10 to the upstream boundary (fig. 18). On the west edge of the flood plain, maximum backwater of 0.3 ft occurs near the mouth of Gum Bayou. Backwater is 0.1 ft at Davis Landing (table 13).

Comparison of figures 18 and 19 shows that upstream from I-10 backwater decreases more rapidly in the upstream direction on the west side of the flood plain than on the east side. On the west side of the flood plain at the upstream boundary, backwater is eliminated, but 0.3 ft of backwater still exists on the east side. On the east side of the flood plain, 0.2 ft of backwater exists from I-10 to the downstream boundary. Although reduced in comparison with the calibration simulation, drawdown still exists downstream from the West Pearl River bridge opening at I-10.

On the basis of the above discussion, alternative 2 can be examined using the previously mentioned objectives. Alternative 2 reduces backwater to the extent that the overtopping of the I-10 crossing is eliminated. The average velocities are reduced on the overbanks and in all main channels. The greatest reduction in average velocity occurs at the Middle River, but the highest average velocity still occurs there.

Alternative 3 Simulation

Alternative 3 differs from alternative 2 in that the cleared area adjacent to the new bridge opening is eliminated. The only difference in the simulations of alternatives 2 and 3 is the value of the Chézy coefficient assigned to the area surrounding the new bridge opening. Therefore, the difference in the computed water-surface elevations between alternatives 2 and 3 is the effect produced by clearing.

Network and Parameter Modifications

The network used in the alternative 2 simulation was also used in the alternative 3 simulation. As in alternative 2, a new 2,000-ft bridge was placed in the I-10 embankment by adding elements to the area of the em-

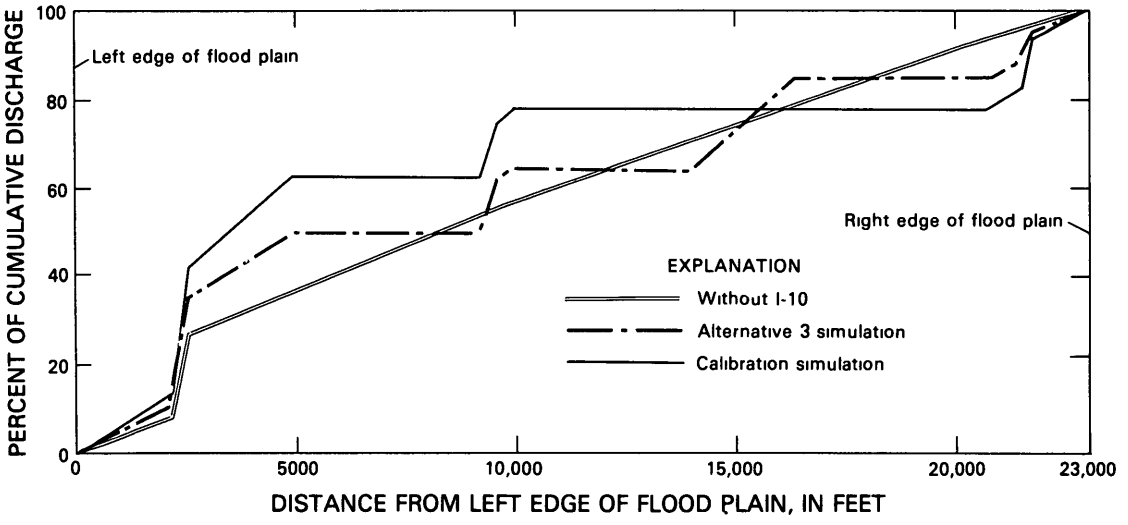

Figure 25. Distribution of discharge across the flood plain at Interstate Highway 10 for alternative 3

bankment occupied by the new bridge (fig. 20). Ground-surface elevations at nodes in the new bridge right-of-way were set at sea level. Ground-surface elevations at nodes in the existing bridge rights-of-way remained the same as those used in the calibration simulation. The Chézy coefficients of elements in the new bridge right-of-way were assigned a value of 40 $ft^{1/2}/s$ (table 12). At the Pearl, Middle, and West Pearl Rivers, the Chézy values (ranging from 21 to 40 $ft^{1/2}/s$) that were used in this simulation were identical to those used in the calibration simulation (table 12). The cleared area adjacent to the new bridge was assigned a Chézy value of 22 $ft^{1/2}/s$ in this simulation; in alternative 2 it was assigned the value of 40 $ft^{1/2}/s$.

Results of the Simulation

The plot of the velocity-vector field for alternative 3 is shown on plate 5 The vector field closely resembles the vector fields obtained from the simulation of alternative 2 and the simulation without I-10 in place. As in other alternatives, the velocity vectors in this simulation have a more southerly component; the southeasterly component, indicating movement toward the Pearl River, does not begin as far upstream as it did in the full-study calibration simulation

The computed cumulative discharge is plotted as a function of distance across the flood plain for simulations with I-10, without I-10, and alternative 3 in figure 25 The distribution of flow across the flood plain closely corresponds to that for alternative 2 (fig. 21) The computed water-surface elevations are shown by contours on plate 5, and values for selected locations are listed in table 13. Upstream from I-10, computed water-surface elevations range from 0.8 to 1.1 ft lower than the computed water-surface elevations with the I-10 embankments in place The water-surface elevation is 1.0 ft higher at Davis Landing, on the west side of the flood plain, than at Napoleon, on the east side. At River Gardens, the subdivision sustaining the heaviest damage in the April 2, 1980, flood, the computed water-surface elevation is 11.7 ft above sea level, 1.1 ft lower than the computed water-surface elevation in the full-study calibration simulation. Upstream at Davis Landing, the computed water-surface elevation is 13.0 ft above sea level, 0.8 ft lower than the elevation obtained in the full-study calibration simulation.

The discharge distribution through the four bridge openings in the I-10 embankment is tabulated in table 14. Discharge decreases at the Pearl, Middle, and West Pearl Rivers (as a percentage of the computed discharge in the calibration simulation) by 22, 34, and 36 percent, respectively. The new bridge placed in the I-10 embankment carries 23 percent of the total computed discharge As in alternative 2, the Pearl River is the major contributor of discharge to the new bridge, on a percentage basis, however, the Middle and West Pearl Rivers are the largest contributors to the new bridge

At the existing bridge openings the reduction in discharge is greatest on the overbanks. This decrease is especially evident at the Middle River, where, as a percentage of the discharge computed in the calibration simulation, discharge decreases 35 percent on both overbanks, and at the West Pearl River, where the discharge

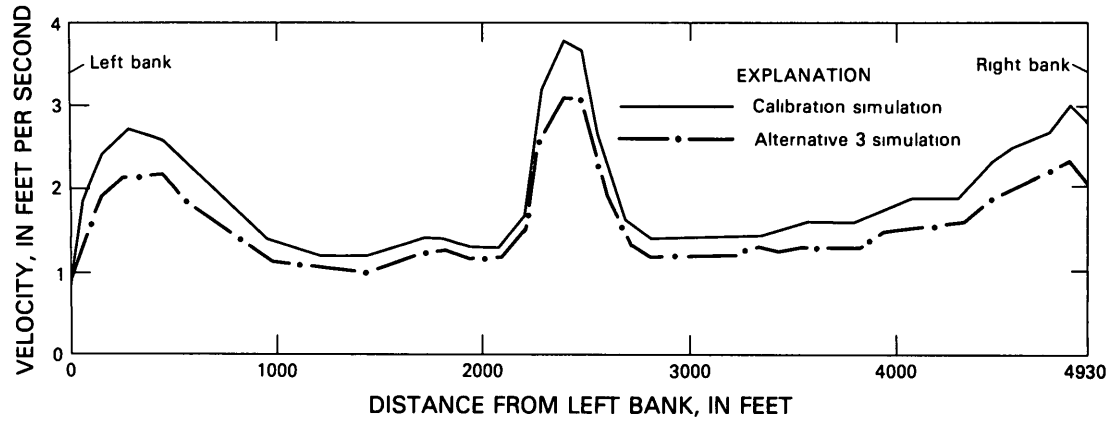

Figure 26. Computed average velocities for the calibration and alternative 3 simulations at the Interstate Highway 10 bridge opening at the Pearl River

decreases on the left and right overbanks by 40 and 37 percent, respectively.

The average velocities for the alternative 3 simulation are plotted in figures 26, 27, and 28 There is a uniform reduction in velocity of 0.3 ft/s on the left and right overbanks of the Pearl River. Relatively large reductions in average velocity occur on the left overbank (0.8 ft/s) and right overbank (0 9 ft/s) of the Middle River. The average velocity in the main channel at the Middle River is 1.3 ft/s lower than the average velocity computed in the calibration simulation. The average velocity is greater on the left overbank than on the right overbank at the West Pearl. The average velocities increase or remain the same in the existing bridge openings compared with alternative 2, but the average velocity in the new bridge opening is 1.9 ft/s, 0.1 ft/s less than that computed in alternative 2. The lower average velocity is caused by the increase in the roughness coefficient on the 1,000- by 3,000-ft area that was cleared of brush and trees in the alternative 2 simulation.

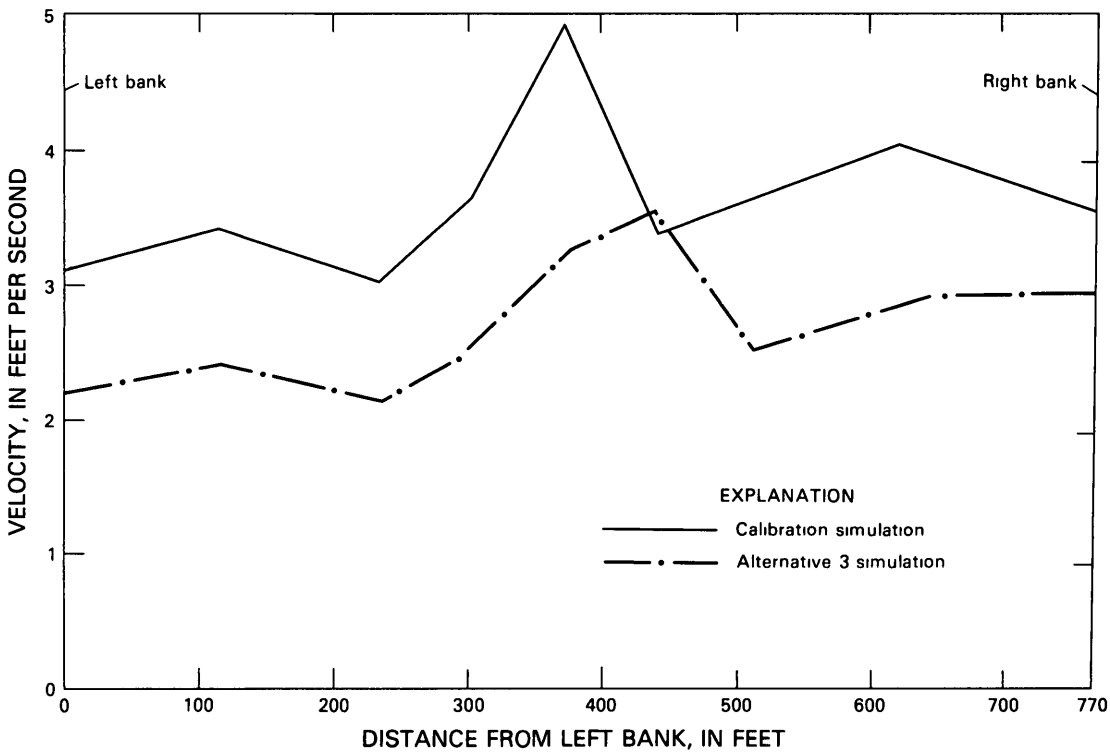

Figure 27. Computed average velocities for the calibration and alternative 3 simulations at the Interstate Highway 10 bridge opening at the Middle River

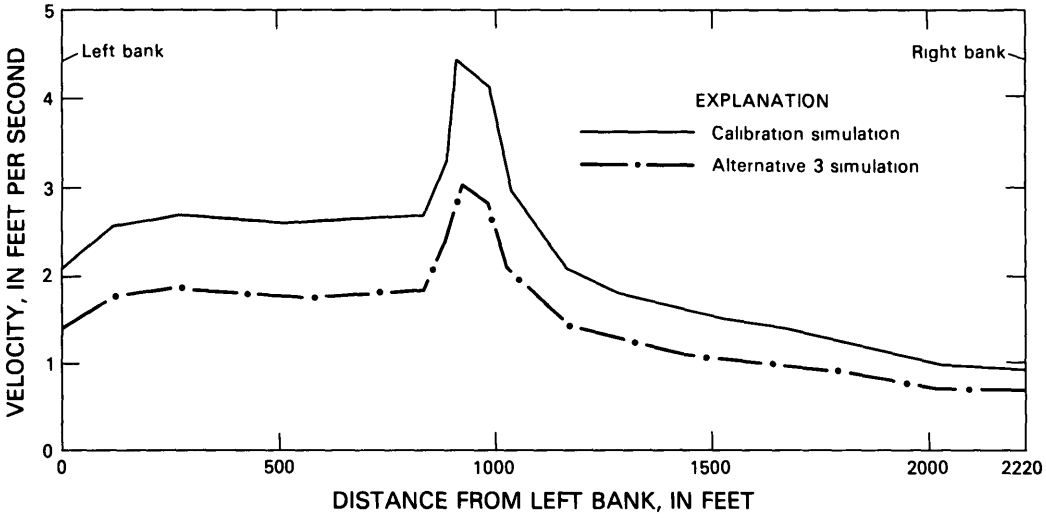

Figure 28. Computed average velocities for the calibration and alternative 3 simulations at the Interstate Highway 10 bridge opening at the West Pearl River

Lines of equal backwater and drawdown are shown on plate 6, and values for selected locations are listed in table 13. Maximum backwater of 0.8 ft occurs along the upstream side of the embankment between the Pearl and Middle Rivers. In the calibration simulation, maximum backwater of 2.1 ft occurred between the Middle and West Pearl Rivers. Along the western margins of the flood plain upstream from I-10, the maximum backwater is 0.3 ft, and at the upstream boundary, backwater is less than 0.1 ft. On the east side of the flood plain, the maximum backwater is 0 3 ft and extends from just upstream from I-10 to the upstream boundary As in the other three alternatives, comparison of figures 18 and 19 indicates that backwater decreases more rapidly in the upstream direction on the west side of the flood plain upstream from I-10 than on the east side. Downstream from I-10, backwater exists on the east side of the flood plain and drawdown on the west side

On the basis of the objectives selected to analyze the alternative modifications, alternative 3 reduces backwater to a fraction of that obtained in the calibration simulation. This reduction in backwater prevents overtopping of I-10 for the flood of April 2, 1980. The average velocities are reduced in all bridge openings, with the highest average velocity occurring in the Middle River opening.

Alternative 4 Simulation

In the alternative 4 simulation, a new 1,000-ft bridge opening was placed in the I-10 embankment. This new bridge was centered along the I-10 embankment in the same location as the 2,000-ft bridge opening used in alternatives 2 and 3. Two main results were obtained using this simulation: (1) the reduction in backwater caused by the addition of a 1,000-ft bridge opening was determined, and (2) the incremental effect of decreasing the new bridge opening from 2,000 to 1,000 ft was determined by comparing alternatives 3 and 4.

Network and Parameter Modifications

The new 1,000-ft bridge opening was added to the I-10 embankment between the Middle and West Pearl Rivers by adding elements to the area occupied by the embankment (fig. 29). The elements located in the new bridge right-of-way were assigned a Chézy value of 40 $ft^{1/2}/s$ (table 12) Ground-surface elevations at nodes in the new bridge right-of-way were set at sea level. At the three existing bridge openings, ground-surface elevations and Chézy values were the same as those used in the full-study calibration simulation. Outside of the new bridge right-of-way, the ground-surface elevations and the values of the Chézy roughness coefficients were identical to those used in the calibration simulation

Results of the Simulation

Water-surface elevations and velocity vectors for alternative 4 are shown on plate 7. As in the other alternative simulations, the velocity-vector field has a more southerly flow component than that obtained in the calibration simulation. This shift in the velocity-vector field indicates that the transfer of flow across the flood

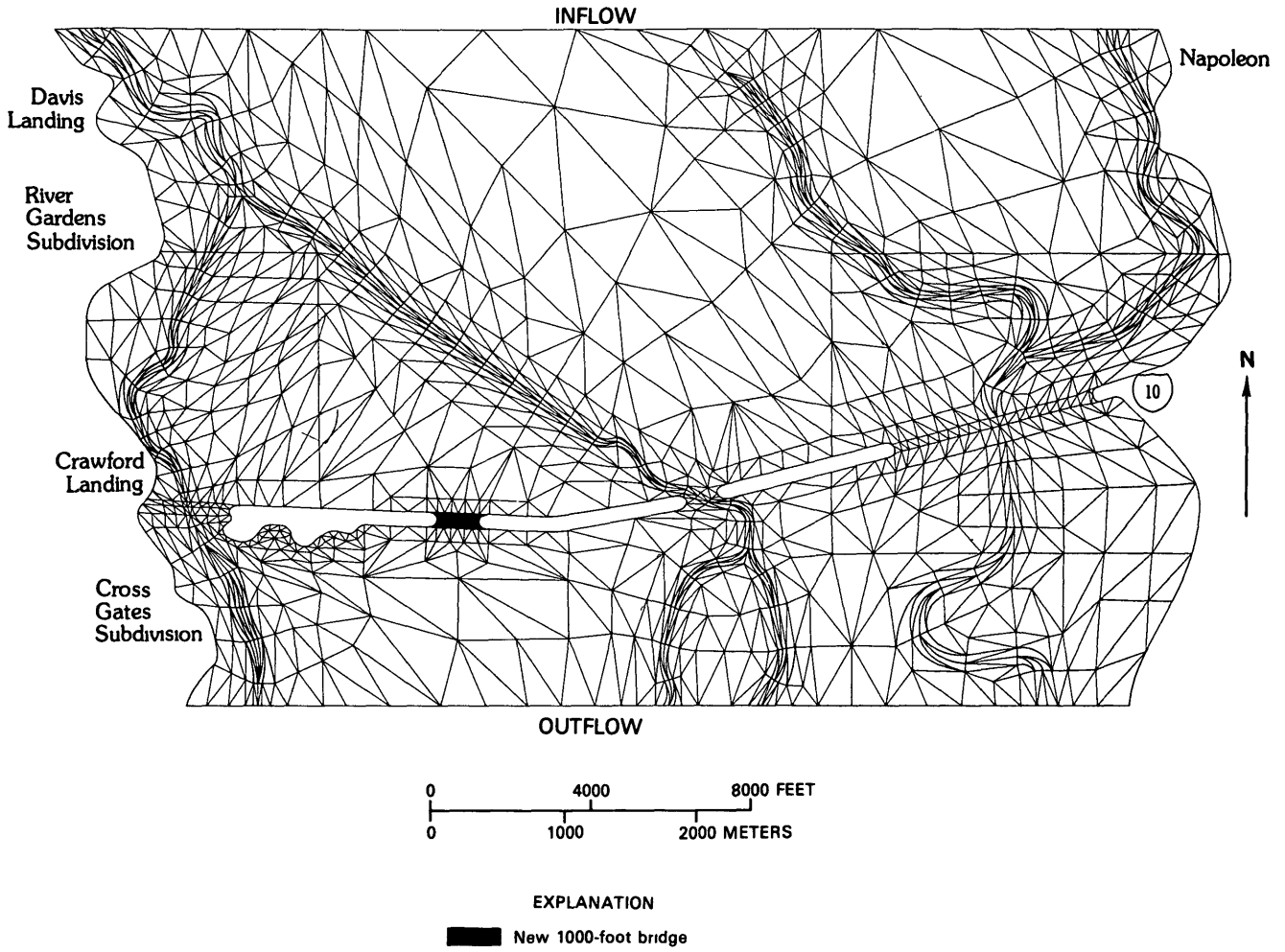

Figure 29. Finite-element network for the alternative 4 simulation

plain does not begin as far upstream from I-10 in this simulation as it did in the calibration simulation.

The computed water-surface elevations are shown by contours on plate 7, and values for selected locations are given in table 13. The steepest water-surface gradients occur through the Middle River and new bridge openings. At the upstream boundary, the water-surface elevation is 1 0 ft higher on the west side of the flood plain than on the east side. Downstream from I-10, water-surface elevations are higher on the east side of the flood plain and lower on the west side than those computed without the highway embankments in place

The computed cumulative discharge is plotted as a function of distance across the flood plain for simulations with I-10, without I-10, and for alternative 4 in figure 30, and the computed discharges through the four bridge openings are tabulated in table 14. Although the discharge through the Pearl River opening is greater than that obtained without I-10 in place, it is less than the discharge through I-10 obtained in the full-study calibration simulation The Pearl River bridge opening and the new bridge opening convey 125,000 ft^3/s, or 73 percent of the total computed discharge.

Discharge decreases through the Pearl, Middle, and West Pearl Rivers (as a percentage of the computed discharge in the calibration simulation) by 19, 29, and 30 percent, respectively. As in alternative 3, the decrease in discharge is greatest on the overbanks, especially at the Middle River, where discharge decreases 30 percent on both overbanks, and at the West Pearl River, where discharge decreases 33 and 32 percent on the left and right overbanks, respectively. In the main channel, discharge decreases 17, 28, and 27 percent at the Pearl, Middle, and West Pearl Rivers, respectively. The new bridge opening

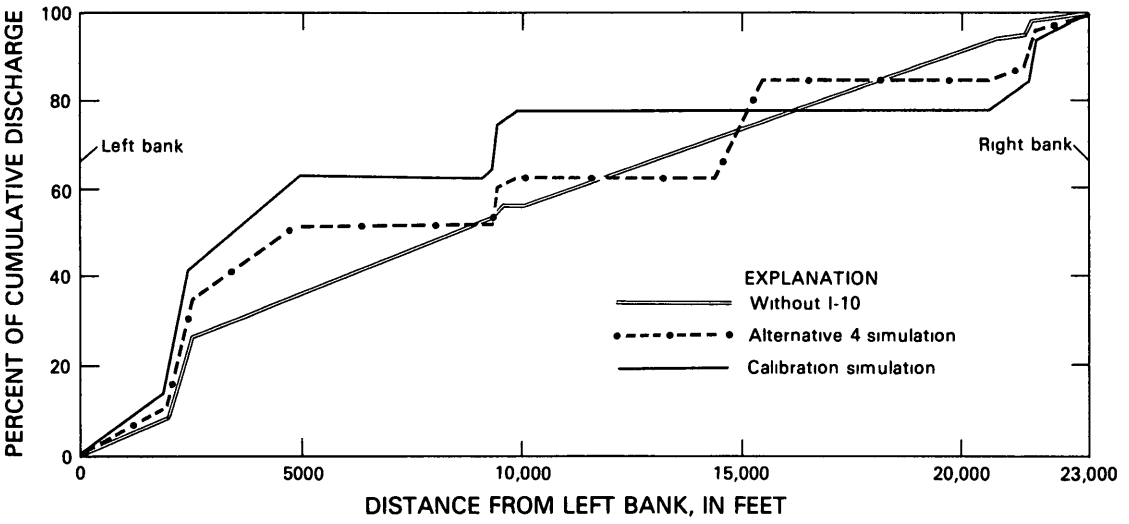

Figure 30. Distribution of discharge across the flood plain at Interstate Highway 10 for alternative 4

conveys 21 percent of the total computed discharge. The greatest share of the 36,600 ft^3/s conveyed by the new bridge comes from the Pearl River opening.

The average velocities through the existing bridge openings are shown in figures 31 to 33. A slight reduction in average velocity of 0.2 ft/s occurs on both overbanks of the Pearl River. The largest reduction in average velocities occurs at the Middle and West Pearl bridge openings. At the Middle River the average velocity decreases 0.7 ft/s and 0.8 ft/s on the left and right overbanks, respectively. At the West Pearl River the average velocity decreases 0.6 ft/s on the left overbank and 0.4 ft/s on the right overbank In the main channel the average velocity decreases 1.1 ft/s at the Middle River and 0.9 ft/s at the West Pearl River. This decrease in average velocity at the existing bridge openings is caused solely by the addition of the new bridge opening, as no other embankment modifications of the highway crossing were made. The average velocity in the new bridge opening is 3.4 ft/s.

Lines of equal backwater and drawdown are shown on plate 8. Values of backwater for selected locations numbered on plate 8 are listed in table 13. The maximum backwater of 0.9 ft occurs along the upstream side of the embankments between the Pearl and Middle Rivers and between the Middle River and the new bridge. Maximum backwater along the west edge of the flood plain is 0 5 ft near River Gardens; on the east side, maximum backwater of 0.4 ft extends from just upstream from I-10 to the upstream boundary of the model. In addition to the upstream backwater, 0.3 ft of backwater extends 0.7 mi downstream from I-10 along the east side of the flood plain. Along the western margins of the flood plain, drawdown exists downstream from I-10 Comparison of

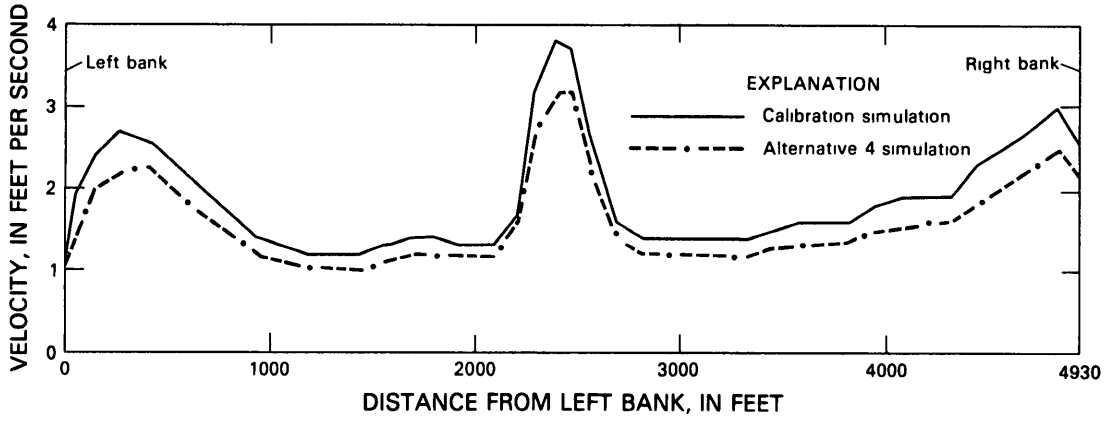

Figure 31. Computed average velocities for the calibration and alternative 4 simulations at the Interstate Highway 10 bridge opening at the Pearl River

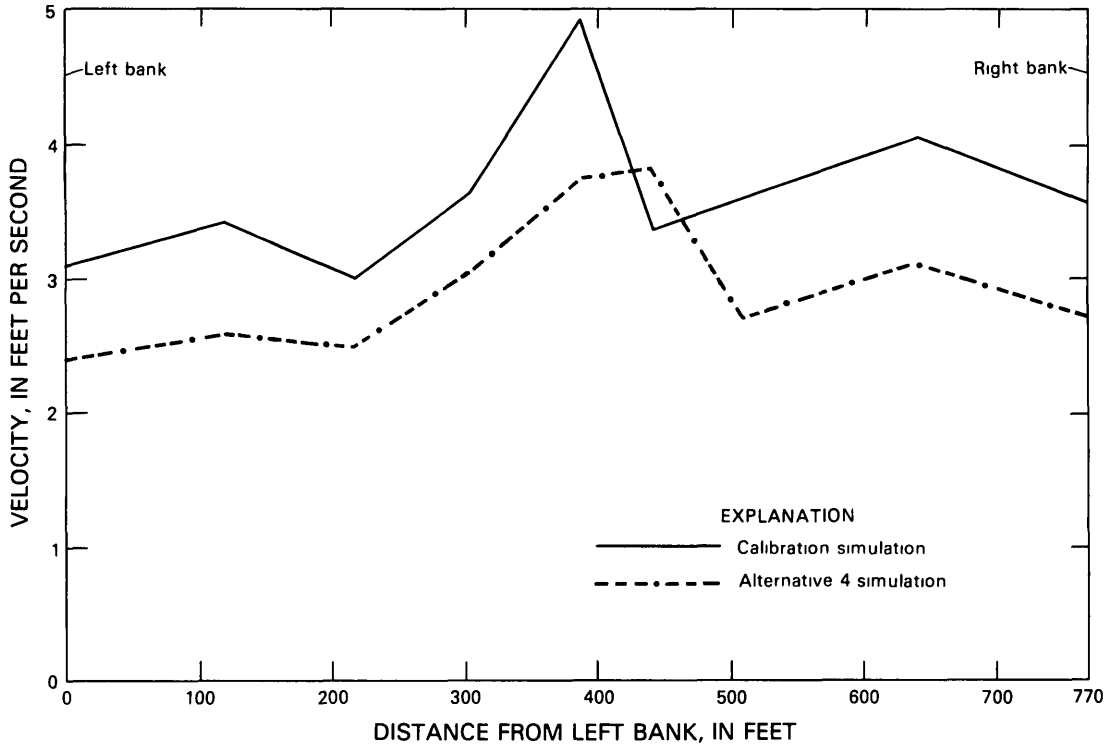

Figure 32. Computed average velocities for the calibration and alternative 4 simulations at the Interstate Highway 10 bridge opening at the Middle River

figures 18 and 19 indicates that backwater upstream from I-10 is greater on the west side of the flood plain than on the east, but the reduction in backwater occurs more rapidly in the upstream direction on the west side than on the east.

Simulation of alternative 4 produces beneficial results, based on the objectives selected for analysis. Backwater is reduced from 1.4 ft to 0.5 ft upstream from I-10 at the mouth of Gum Bayou, thereby preventing the overtopping of I-10 for a flood such as the one that occurred in 1980. Although not eliminated, backwater is reduced downstream from I-10 on the east edge of the flood plain. Drawdown increases slightly, on the west edge of the flood plain 0.2 mi downstream from I-10, from -0.1 ft in the calibration simulation to -0.2 ft in this alternative. Finally, the average velocities are reduced in all the existing bridge openings.

Comparison of Alternatives

In the presentation of the alternatives, comparisons have been made between each alternative simulation and the full-study calibration simulation. Additional comparisons of the alternative simulations need to be discussed. Two comparisons that provide valuable information are: (1) by comparing alternatives 2 and 3, the effect of the cleared area at the new bridge opening is obtained; and (2) by comparing alternatives 3 and 4, the effect of increasing the new bridge opening from 1,000 to 2,000 ft is obtained. These two comparisons will aid highway planners in evaluating the incremental effects obtained by clearing or increasing the width of the bridge opening.

The new 2,000-ft bridge opening without clearing (alternative 3) conveys 38,700 ft^3/s, 23 percent of the total computed discharge (table 14). With the addition of the cleared area (alternative 2), the discharge through the new bridge increases to 41,000 ft^3/s, or 25 percent of the total computed discharge. Thus, clearing increases the discharge through the new bridge by 2,300 ft^3/s.

The average velocities for alternatives 2 and 3 are shown in table 15. As indicated in this table, the average velocities at the Pearl and West Pearl Rivers remain unchanged between alternatives 2 and 3. At the Middle River, the velocity is slightly lower with clearing than without. At the new bridge the average velocity is 0.1 ft/s higher with clearing than without.

The computed water-surface elevations and backwater for selected locations are listed in table 13.

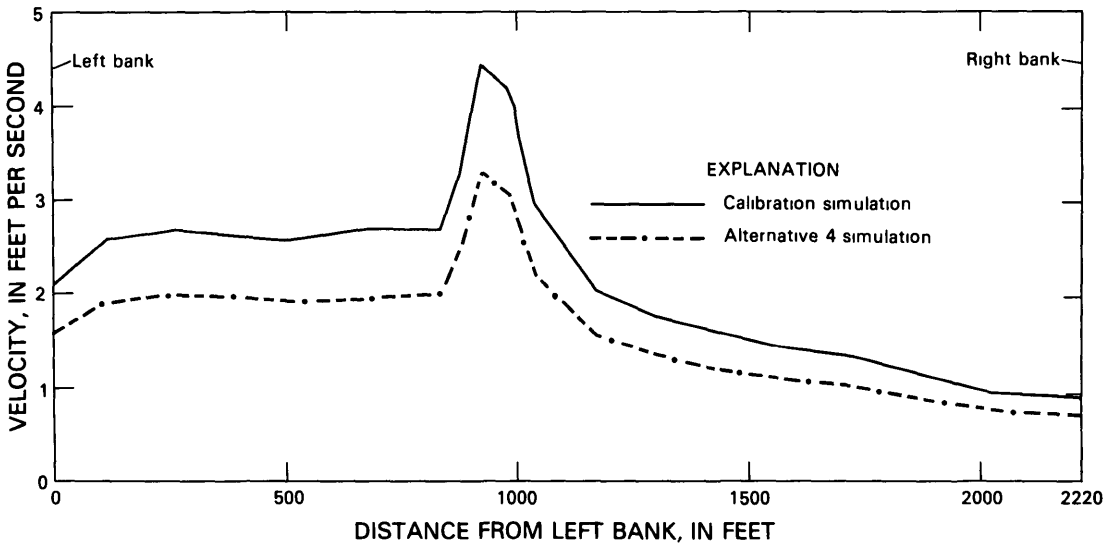

Figure 33. Computed average velocities for the calibration and alternative 4 simulations at the Interstate Highway 10 bridge opening at the West Pearl River

Comparisons of alternatives 2 and 3 in the table and comparison of plates 4 and 6 show that clearing has minimal effect on backwater along the edges of the flood plain The computed water-surface elevations for the center of the channel at the Pearl and West Pearl Rivers are shown in figures 18 and 19. The addition of the cleared area in alternative 2 produces less than 0.1 ft of reduction in water-surface elevation (the difference between the lines for alternatives 2 and 3).

In alternative 3 the 2,000-ft bridge opening conveys 38,700 ft^3/s, and in alternative 4 the 1,000-ft bridge conveys 36,600 ft^3/s (table 13) Thus, the 1,000-ft bridge conveys 2,100 ft^3/s less than the 2,000-ft opening. To convey this discharge through the 1,000-ft opening, an increase in average velocity from 1.9 ft/s in alternative 3 to 3.4 ft/s in alternative 4 occurs (table 5). The higher velocity in the 1,000-ft bridge opening is associated with a large water-surface gradient through the opening. At the existing bridge openings, average velocities are 0.1 to 0.2 ft/s higher in alternative 4 than in alternative 3.

The lines of equal backwater and drawdown for alternatives 3 and 4 are shown on plates 6 and 8, respectively, and values for selected locations are listed in table 13. On the west side of the flood plain, backwater is 0.2 ft greater at the mouth of Gum Bayou and at River Gardens with the new 1,000-ft bridge opening (alternative 4) than with a new 2,000-ft bridge opening (alternative 3). At Davis Landing, backwater is 0.1 ft greater in alternative 4 than in alternative 3. Downstream from I-10 on the east side of the flood plain, backwater is 0.1 ft greater in alternative 4 than in alternative 3. Downstream from I-10 on the west side of the flood plain, drawdown is the same in alternatives 3 and 4.

SUMMARY AND CONCLUSIONS

Lee and others (1983) indicated that a combination of natural and manmade factors causes water to flow across the Pearl River flood plain from the higher west side to the lower east side with or without I-10 in place. However, with the roadway in place, the shift of flow from west to east occurs farther upstream. Upstream from I-10, maximum backwater is greater at the west edge of the flood plain than at the east edge. Accompanying the roadway-induced shift of flow to the east are higher water-surface elevations downstream from the roadway in the eastern part of the flood plain and lower water-surface elevations downstream in the western part

The two-dimensional finite-element surface-water flow-modeling system, FESWMS, was used to study the effect of alternatives for improving the hydraulic characteristics of the I-10 crossing of the flood plain of the Pearl River near Slidell, La. The analyses used the model's capability to simulate changes in flood-plain topography, flood-plain vegetative cover, and highway-embankment geometry.

On the basis of the results of Lee and others (1983), a local model of the West Pearl River bridge opening was developed to make comparisons among seven possible alternative modifications of the I-10 highway crossing that range from clearing of vegetation to removal of spoil and

installation of culverts. The local model showed that two greatly different modifications of the highway crossing can produce similar reductions in both backwater and average velocity. Also, comparison of different alternatives shows that the same reduction in backwater can be obtained with different average velocities or, conversely, the same average velocities can be obtained with different reductions in backwater.

A larger network and modifications to it were used to analyze four alternate modifications of the I-10 crossing.

The average velocities in the main channels and on the overbanks at the existing bridge openings decrease in structural alternatives 2, 3, and 4 (new bridge). Alternative 1, the nonstructural alternative (clearing of vegetation and removal of spoil), produces overall reductions in average velocities through the bridge openings, but somewhat higher average velocities occur on the overbanks of the Middle River. The average velocity in the new bridge opening is lowest in alternative 2 and highest in alternative 4.

As in the simulation without I-10, the four alternatives that were simulated produce higher water-surface elevations on the west side of the flood plain than on the east side upstream from I-10. As a result, transfer of water across the flood plain does not occur as far upstream from I-10 in the four alternative simulations as it did in the calibration simulation (based on the April 2, 1980, flood). Downstream from I-10, computed water-surface elevations are higher on the east side of the flood plain than on the west side, although they are lower than the values computed in the calibration simulation.

Backwater is reduced from values obtained in the calibration simulation in all the alternative simulations. At River Gardens subdivision on the west side of the flood plain, 1.4 ft of backwater existed with I-10 in place, whereas in the alternative simulations backwater ranges from 0.5 to 0.2 ft. On the west side of the flood plain, drawdown remains the same in alternative 1 (0.1 ft) as in the calibration simulation but increases to 0.3 ft in alternatives 2 and 3.

Some generalizations can be made on the basis of the results of this study. Both structural and nonstructural modifications of highway crossings of wide flood plains can have significant beneficial effects on the hydraulic characteristics of such crossings. A nonstructural approach can result in reduced backwater and lower overall bridge-opening velocities, even with an increased discharge through an opening. Structural approaches can provide a greater reduction in backwater than a nonstructural approach and can significantly reduce velocities in existing bridge openings. The three structural and one nonstructural modifications provide planners with a range of options to improve the hydraulic characteristics of the I-10 crossing.

REFERENCES

Cardwell, G. T., Forbes, M. J., Jr., and Gaydos, M. W., 1967, Water resources of the Lake Pontchartrain area, Louisiana: Louisiana Department of Conservation and Louisiana Department of Public Works Water Resources Bulletin 12, 105 p.

Chow, V. T., 1959, Open-channel hydraulics: New York, McGraw-Hill, 680 p.

Gee, D. M., and MacArthur, R. C., 1978, Development of generalized free surface flow models using finite element techniques, *in* Brebbia, C. A., and others, eds., Finite elements in water resources: International Conference on Finite Elements in Water Resources, 2d, London 1978, Proceedings, London, Pentech Press, p. 2.61-2.79.

———1982, Evaluation and application of the generalized finite element hydrodynamic model, RMA-2, *in* MacArthur, R. C., and others, eds., Two-Dimensional Flow Modeling: U.S. Army Corps of Engineers--Sponsored Seminar on Two-Dimensional flow modeling, 1st, Davis, Calif., 1981, Proceedings, Davis, Calif., U.S. Army Corps of Engineers, The Hydrologic Engineering Center, p. 97-109.

Hood, P., 1976, Frontal solution program for unsymmetric matrices: International Journal for Numerical Methods in Engineering, v. 10, no. 2, p. 379-399.

———1977, Note on frontal solution program for unsymmetric matrices: International Journal for Numerical Methods in Engineering, v. 11, no. 6, p. 1055.

King, I. P., and Norton, W. R., 1978, Recent applications of RMA's finite element models for two-dimensional hydrodynamics and water quality, *in* Brebbia, C. A., and others, eds., Finite elements in water resources: International Conference on Finite Elements in Water Resources, 2d, London 1978, Proceedings, London, Pentech Press, p. 2.81-2.99.

Lee, F. N., and Arcement, G. J., 1981, Hydrologic analysis of Pearl River floods, April 1979 and April 1980, in Louisiana and Mississippi: Louisiana Department of Transportation and Development, Office of Highways, Research Study 81-1-SS, 37 p.

Lee, J. K., 1980, Two-dimensional finite element analysis of the hydraulic effect of highway bridge fills in a complex flood plain, *in* Wang, S. Y., and others, eds., Finite elements in water resources: International Conference on Finite Elements in Water Resources, 3d, University, Miss., 1980, Proceedings, University, Miss., University of Mississippi, School of Engineering, p. 6.3-6.23.

Lee, J. K., and Bennett, C. S., III, 1981, A finite-element model study of the impact of the proposed I-326 crossing on flood stages of the Congaree River near Columbia, South Carolina: U.S. Geological Survey Open-File Report 81-1194, 56 p.

Lee, J. K., Froehlich, D. C., Gilbert, J. J., and Wiche, G. J., 1983, A two-dimensional finite-element model study of backwater and flow-distribution at the I-10 crossing of the Pearl River near Slidell, Louisiana: U.S. Geological Survey Water-Resources Investigations Report 82-4119, 60 p.

Norton, W. R., and King, I. P., 1973, A finite element model for Lower Granite Reservoir, computer application supple-

ment and user's guide· Walnut Creek, Calif, Water Resources Engineers, Inc., 90 p

Norton, W R, King, I. P, and Orlob, G. T, 1973, A finite element model for Lower Granite Reservoir: Walnut Creek, Calif, Water Resources Engineers, Inc., 138 p

Pinder, G. F, and Gray, W G, 1977, Finite element simulation in surface and subsurface hydrology New York, Academic Press, 295 p

Pritchard, D W, 1971, Two-dimensional models, *in* Ward, G H, Jr, and Espey, W H, Jr, eds., Estuarine modeling--An assessment Washington, DC, Environmental Protection Agency, Water Quality Office, Water Pollution Control Research Series 16070DZV, p 22-33

Shell, J D, compiler, 1981, Drainage areas in the Pearl River basin, Mississippi-Louisiana, pt. 2, Pearl River below Strong River to mouth Jackson, Miss, US Geological Survey, 232 p

Tseng, M T, 1975, Evaluation of flood risk factors in the design of highway stream crossings, v III, Finite element model for bridge backwater computation Washington, DC, Federal Highway Administration, Report FHWD-RD-75-53, 176 p

US Army Corps of Engineers, 1981, Pearl River basin reconnaissance report (stage 1 report) Mobile, Ala, US Army Corps of Engineers, 200 p

US Geological Survey, 1981, Water resources data for Mississippi. US Geological Survey Water-Data Report MS-79-1, 438 p

———1983, Water resources data for Louisiana, water year 1982, v 2, Southern Louisiana. US Geological Survey Water-Data Report LA-82-2, 404 p.

US Water Resources Council, 1977, Guidelines for determining flood flow frequency Washington, D.C., U.S Water Resources Council, Hydrology Committee, Revised Bulletin 17A, 163 p

Walters, R A, and Cheng, R. T, 1978, A two-dimensional hydrodynamic model of a tidal estuary, *in* Brebbia, C A, and others, eds, Finite elements in water resources International Conference on Finite Elements in Water Resources, 2d, London 1978, Proceedings, London, Pentech Press, p 2 3-2 21.

———1980, Accuracy of an estuarine hydrodynamic model using smooth elements Water Resources Research, v 16, no 1, p 187-195

Wax, C L, and Tingle, J L, 1980, The Pearl River flood of Easter 1979--A water balance explanation Mississippi State, Miss, Mississippi State University, Water Resources Research Institute, 27 p

Zienkiewicz, O C, 1977, The finite element method (3d ed.) London, McGraw-Hill, 787 p.

METRIC CONVERSION FACTORS

Multiply	By	To obtain
ft (foot)	0 3048	m (meter)
ft/s (foot per second)	0 3048	m/s (meter per second)
ft/s^2 (foot per second squared)	0 3048	m/s^2 (meter per second squared)
ft^3/s (cubic foot per second)	0 02832	m^3/s (cubic meter per second)
mi (mile)	1 609	km (kilometer)
mi^2 (square mile)	2 590	km^2 (square kilometer)
ft/mi (foot per mile)	0 1894	m/km (meter per kilometer)
$slug/ft^3$ (slug per cubic foot)	515 4	kg/m^3 (kilogram per cubic meter)
$lb \cdot s/ft^2$ (pound second per square foot)	478 7	Pa·s (pascal second)

National Geodetic Vertical Datum of 1929 (NGVD of 1929) A geodetic datum derived from a general adjustment of the first-order level nets of both the United States and Canada, formerly called mean sea level, is referred to as sea level in this report